GROUND STATE STRUCTURE, DOMAIN WALLS, AND EXTERNAL FIELD RESPONSE IN RANDOM MAGNETS

Eira Seppälä

Laboratory of Physics
Helsinki University of Technology

Fysiikan laboratorio
Teknillinen korkeakoulu

DISSERTATION 112 (2001)

GROUND STATE STRUCTURE, DOMAIN WALLS, AND EXTERNAL FIELD RESPONSE IN RANDOM MAGNETS

Eira Seppälä

Laboratory of Physics
Helsinki University of Technology
Espoo, Finland

Dissertation for the degree of Doctor of Science in Technology to be presented with due permission of the Department of Engineering Physics and Mathematics, Helsinki University of Technology for public examination and debate in Auditorium E at Helsinki University of Technology (Espoo, Finland) on the 25th of May, 2001, at 12 o'clock noon.

Dissertations of Laboratory of Physics, Helsinki University of Technology
ISSN 1455-1802

Dissertation 112 (2001):
Eira Seppälä: Ground State Structure, Domain Walls, and External Field Response in Random Magnets
ISBN 951-22-5458-1 (print)
ISBN 951-22-5459-X (electronic)

OTAMEDIA OY
ESPOO 2001

Abstract

The ground state structure and domain walls in Ising-like magnets with quenched randomness are studied at zero temperature. The methods employed are exact ground state calculations using graph-theoretical optimization and extreme statistics arguments.

The elastic manifolds, *i.e.*, domain walls, with random-bond disorder are investigated with two different types of periodicity. The first type of periodicity is when the randomness is periodically repeated. It is shown to lead after a cross-over to the periodic elastic media universality class, whenever the period λ is finite. The second periodicity is due to an additional modulating potential. There are two types of intermittence seen before the asymptotic random-bond roughness behavior is reached. The first type is when the manifolds jump between the minima of the periodic potential and the second type is when the interfaces roughen over pinning energy barriers.

An external field is applied to the random manifolds. An energy minimization argument based on the glassy energy landscape indicates that in an equilibrium system the manifolds move by sharp jumps between nearly degenerate energy minima in analogy to a first-order transition. A mean field argument for the finite-size scaling of the first jump field is derived and numerically confirmed. Using extreme statistics and probabilistic arguments, the probability distribution of the first jump field and its finite size scaling are calculated. Based on these the susceptibility of the manifolds is derived.

Random field magnets are studied in two dimensions. The break-up of long-range order is shown to have a first-order character. The domain wall behavior is studied, leading to an interface scaling with a roughness exponent greater than unity below the break-up length scale. The domain wall energy is demonstrated to vanish logarithmically confirming the destruction of the long-range order. The magnetization and susceptibility versus the external field are investigated, and they show continuous behaviors and are independent of the break-up length scale. However, another long-range order, percolation, is found in two-dimensional random field magnets. The percolation transition with respect to the external field belongs to the standard short-range correlated two-dimensional percolation universality class. The whole phase diagram for percolation as a function of the random field strength and the external field is predicted.

Preface

This thesis has been prepared in the Laboratory of Physics at the Helsinki University of Technology during the years 1997-2001.

I wish to thank my advisor Docent Mikko Alava for his inspiring, active, and intensive guidance during these years. Working with Mikko is never boring, but interesting and mostly fun. His contribution in my graduate studies has been crucial. I would also like to thank Academy Professor Risto Nieminen for giving me the opportunity to undertake this thesis. Risto has brought up a large and active research group with excellent facilities, which very well support the research done in the group. I am grateful to Professor Phil Duxbury for the inspiring and fruitful collaboration. Visiting Phil at the Michigan State University has always been fun and profitable. In addition I would like to thank Mr. Viljo Petäjä and the others of the disordered materials group, Dr. Simone Artz, Mr. Erkki Hellén, Dr. Vilho Räisänen, and Mr. Lauri Salminen, for collaboration and useful conversations. There are many people all around the world from whom I have learned a great deal while preparing the thesis. I should especially mention and thank Dr. Cristian Moukarzel and Professor Heiko Rieger for nice and educative discussions. In the Laboratory of Physics there are so many nice people that I cannot name them all here, but I do need to mention and thank Professors Martti Puska and Kimmo Saarinen for collaboration in teaching and good advice, and Dr. Andrés Auyela for his contribution to the great atmosphere in the laboratory. I am also grateful to the rest of my friends, especially JRBS, and to my sister, brother, and both of my parents. This work is dedicated to my father, who probably has the most crucial and primal contribution to the fact that I ever ended up studying science.

The last but definitely not least acknowledgments belong to my soon-to-be-husband Oskari, whose patience, support, and understanding is not only incredible at home, but important at work, too.

Otaniemi, May 2001

Eira Seppälä

Contents

List of publications

This thesis consists of an overview and the following publications:

I E. T. Seppälä, M. J. Alava, and P. M. Duxbury, "Periodic elastic medium in which periodicity is relevant", Physical Review E **62**, 3230-3233 (2000).

II E. T. Seppälä, M. J. Alava, and P. M. Duxbury, "Intermittence and roughening of periodic elastic media", Physical Review E **63**, 036126 (2001) (*7 pages*).

III E. T. Seppälä and M. J. Alava, "Energy landscapes in random systems, driven interfaces and wetting", Physical Review Letters **84**, 3982-3985 (2000).

IV E. T. Seppälä, M. J. Alava, and P. M. Duxbury, "Extremal statistics in the energetics of domain walls", Physical Review E (June 2001, 4 pages).

V E. T. Seppälä and M. J. Alava, "Energy landscapes, lowest gaps, and susceptibility of elastic manifolds at zero temperature", accepted for publication in European Physical Journal B.

VI E. T. Seppälä, V. Petäjä, and M. J. Alava, "Disorder, order, and domain wall roughening in the two-dimensional random field Ising model", Physical Review E **58**, R5217-R5220 (1998).

VII E. T. Seppälä and M. J. Alava, "Susceptibility and percolation in two-dimensional random field Ising magnets", Physical Review E (June 2001, 14 pages).

The author has had an active role in all the phases of the research reported in this thesis. She has been actively involved in planning the calculations done, in deriving the analytical calculations, and interpreting the results. She has implemented and written all the used algorithms and computer programs herself, and performed all the numerical calculations and data-analysis except for a small part of the calculations done for Publication VI. The author has written Publications I, IV, V, and VII, and contributed actively to the writing of the other papers.

1 Random Ising Magnets

1.1 Introduction

In statistical mechanics pure magnets offer simple, but rich in their physics, examples of continuous phase transitions including the concepts of universality, broken symmetry, critical phenomena, scaling, and renormalization [1, 2, 3]. The beauty of magnets is that there are a number of experimentally measurable systems available, in which the theories can be tested. On the other hand the physics emerges from simple models and rules. For a long time the experimentalists were forced to do their best in reducing the amount of "dirt" or "junk", *i.e.*, inhomogeneities such as impurities, in samples. However, for about twenty-five years now, since the seminal paper by Imry and Ma [4], the quenched, frozen-in, structural disorder has become a topic of interest in itself, and it has provided many new fascinating phenomena objects of study [5].

Disordered magnets, like the pure magnets of traditional temperature-driven phase transitions, act as good examples of collective phenomena in systems with quenched randomness including models of a few rules and experimental systems with almost in a statistical sense ideal, homogeneous randomness. The term *quenched* is used in order to make a distinction from the *annealed* case [1]. In the annealed case *e.g.* of a lattice of magnetic ions, where non-magnetic impurity atoms are present, the system is cooled from high temperatures slowly, so that the magnetic ions and impurities are in thermal equilibrium with each other. The impurities are able to move and their positions should be traced when calculating the partition function of the system. In the quenched case, however, the impurities are fixed in space in the system. The examples of experimental realizations of random magnets range over a wide area from structural phase transitions and charge-density waves in random alloys, dirty high-temperature superconductors, and fluids in porous media to wetting on disordered substrates [5]. The three most studied classes of randomness in magnets are called *random-exchange*, *random-field*, and *spin glasses*. In this work only the first two are studied.

This thesis consist of studies of ground state structures, domain walls, and external field response in random magnets at zero temperature using mainly exact ground state calculations. The background and some concepts related to random magnets, and the methods used are introduced in this Section. In Section 2 two types of periodicity in elastic manifolds are studied. The

external field response to the domain walls is considered in Section 3 and two-dimensional random field magnets are studied in Section 4.

1.2 Disorder in Magnets

Pure Magnets

For pure magnets the simplest magnetic model is called the Ising or Lenz-Ising model [6], which is described by the classical spin-half Hamiltonian

$$\mathcal{H} = -\sum_{\langle ij \rangle} J_{ij} S_i S_j, \tag{1}$$

where the sum is calculated over all the nearest neighboring spin pairs S_i and S_j, the spins can point "up" $(+\frac{1}{2})$ or "down" $(-\frac{1}{2})$. For pure Ising ferromagnets the coupling constant J is positive and the same for all the nearest neighboring pairs. In the pure case at dimensions greater than unity there exists a phase transition at a critical temperature T_c. Below T_c the systems are ferromagnets, whence the *order parameter* $m \equiv \langle S_i \rangle_t$, which is called the magnetization or the "spontaneous magnetic density", has a nonzero value. The brackets $\langle \dots \rangle_t$ denote thermal equilibrium. Above T_c the entropy wins over the energy, the spins point more or less randomly up or down, and the magnetization vanishes. For one-dimensional magnets $T_c = 0$, *i.e.*, even an infinitesimal temperature makes the systems disordered and only at zero-temperature the magnet is ordered. Thus the so called *lower critical dimension* $d_l = 1$.

Random Magnets

Perhaps the simplest way to have quenched randomness in magnets comes in the form of substitutionally disordered materials in which magnetic and non-magnetic ions are alloyed together. In this case the exchange interactions between pairs vary and are short-range correlated. If the coupling constants are positive (semi-definite), $J_{ij} \geq 0$ in Eq. (1), the system is called the *random-exchange* or *random-bond* Ising model (RBIM). The random-exchange Ising model (REIM) is qualitatively similar to the pure case, *e.g.* the lower-critical dimension remains one. However, the quantitative measures change. When discussing domain walls, see a sketch in Fig. 1, we

will return to random bond (RB) type of randomness, since the domain walls in the REIM differ substantially from the pure case. If there are coupling constants with equal amounts of negative and positive values, $J_{ij} \lesseqgtr 0$, *i.e.*, there are antiferromagnetic and ferromagnetic interactions present, the system is called a *spin glass* [7, 8, 9]. Antiferromagnetic couplings prefer the nearest neighboring spins to be oriented opposite to each other and ferromagnetic interactions prefer the spins to be aligned, and thus there is a competition between ferromagnetic and antiferromagnetic couplings. At low temperatures the spins should satisfy simultaneously all the exchange interactions in the Hamiltonian and they become *frustrated* when failing in it. Hence finding the ground state structure for spin glasses is a highly nontrivial task. Although the spin glass problem comprises a lot of interesting physics and open questions it is not a topic of this thesis.

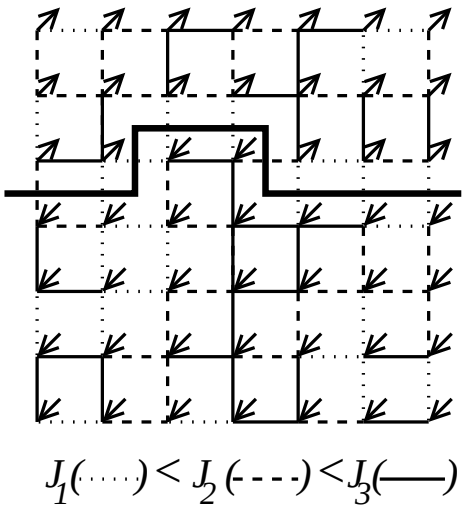

Figure 1: A two-dimensional random exchange magnet with three different positive coupling constant values $J_1 < J_2 < J_3$. The spins in opposite boundaries are fixed to point up and down, and thus there exists a domain wall between the up and down spin domains.

Random Field Magnets

The *random-field* Ising model (RFIM) is defined by the Hamiltonian

$$\mathcal{H} = -J \sum_{\langle ij \rangle} S_i S_j - \sum_i h_i S_i, \tag{2}$$

where the magnetic fields h_i are random and short-range correlated [4, 10, 11]. The random fields (RF) are usually chosen from an even distribution, so that there is a statistically equal number of fields pointing up and down, and the mean is zero. They are normally either taken from a bimodal distribution,

$$P(h_i) = \frac{1}{2}\delta(h_i - \Delta) + \frac{1}{2}\delta(h_i + \Delta), \tag{3}$$

or from a continuous distribution, such as a uniform or a Gaussian distribution,

$$P(h_i) = \frac{1}{\sqrt{2\pi}\Delta} \exp\left[-\frac{1}{2}\left(\frac{h_i}{\Delta}\right)^2\right], \tag{4}$$

where the disorder strength is given by Δ, the standard deviation of the distribution. The ferromagnetic exchange interaction $J > 0$ now competes with the random fields, which prefer to have the spins oriented with the local field.

Experiments on Random Field Magnets

Although it at first glance looks difficult to have experimental systems with the random field type of disorder, there is actually a strikingly rich class of such experimentally accessible disordered systems. The most studied RF system is a diluted antiferromagnet in a field (DAFF), where the combination of dilution and the external field leads to a random field contribution in the staggered magnetization, which is the order parameter for an antiferromagnet. The Hamiltonian of DAFF is

$$\mathcal{H} = -J \sum_{\langle ij \rangle} S_i S_j \epsilon_i \epsilon_j - B \sum_i \epsilon_i S_i, \tag{5}$$

where the coupling constants $J < 0$, ϵ_i is the occupation number of a spin S_i, and B is the constant external field. The Hamiltonian may be transformed to the Hamiltonian of RFIM (2) [12, 13]. One of the best three-dimensional RFIM realizations or DAFFs is $Fe_xZn_{1-x}F_2$, where the magnetic atoms, Fe, are replaced by non-magnetic ones, Zn, with a concentration of $1 - x$ [14]. There are also other type of experimental realizations of RFIM such as wetting of liquid helium on a disordered substrate [15].

The Lower Critical Dimension of RFIM

Imry and Ma used in their introductory paper of the random-field problem a domain argument to show that the lower critical dimension changes from the pure case to $d_l = 2$ [4]. At low temperatures, when the Hamiltonian of the random-field magnets, Eq. (2), is minimized, in order to have a domain of a linear size L the domain wall creates an energy cost of $\mathcal{O}(JL^{d-1})$. On the other hand the system gains energy by flipping the domain from the fluctuations of random fields. The typical fluctuations predicted from Poissonian statistics are $\mathcal{O}(\Delta L^{d/2})$. Thus, whenever $d/2 \geq d-1$, *i.e.*, $d \leq 2$, it is energetically favorable for the system to break into domains. However, field-theory calculations in the late seventies with a dimensional reduction from the random field to the pure case, $d \to d-2$, suggested that the lower critical dimension $d_l = 3$ [16, 17, 18, 19, 20]. On the other hand, studies in the early eighties of the continuum interface in random field systems gave $d_l = 2$ [21, 22]. Also an elaborate calculation by optimizing the domain wall structure by Binder [23] confirmed $d_l = 2$ and showed that the effective ferromagnetism, which exists at small system sizes, vanishes at the length scale

$$L_b \sim \exp[A(J/\Delta)^2], \tag{6}$$

where A is a constant of order unity, see also [24]. Finally first Imbrie and then Bricmont and Kupiainen [25, 26] rigorously proved that there is a ferromagnetic phase in the three-dimensional (3D) random field Ising model. Later Aizenman and Wehr [27] gave a proof that there is no ferromagnetic phase in 2D RFIM, hence d_l was confirmed to be two. In this thesis the random field magnets are studied in two dimensions, and thus such topical issues as the critical exponents of the phase transition in 3D RFIM are not considered [10, 11, 14].

One should note that for the RFIM the order parameter is the magnetization, $\langle m \rangle$, where the brackets now denote the disorder-average over the ensemble of realizations of randomness. A closely related concept is the idea of *self-averaging* [1], which means that the quenched average value of a measure (*e.g.* energy) represents the behavior of a typical sample, when approaching the thermodynamic limit, $L \to \infty$. However, in random systems all the measures are not self-averaging, and one should be careful when dealing with such quantities.

A question, which arises when studying random systems, is when the randomness is strong enough to change the systems' behavior from the pure case. In the *renormalization group* (RG) language the question is whether the impurities are *relevant* at the critical point to change the universality class of the system. The answer to the question is known as the *Harris criterion* [1, 28]. The specific heat exponent α in magnetic systems is related to the dimension d of the system and the spin-spin correlation length exponent ν with a *hyper-scaling relation* (the term "hyper" means that the dimension is included in the scaling relation):

$$\alpha = 2 - d\nu. \tag{7}$$

The Harris criterion tells that the higher order terms generated by the two-point energy correlation in the expansion of the partition function are important and thus the randomness is relevant if $d\nu < 2$, *i.e.*, $\alpha > 0$. This is the case *e.g.* for the three dimensional random bond Ising model. The relevant randomness describes a new, random, fixed point. However, it has been proved that for example in the randomly diluted ferromagnet there are arbitrarily large regions, which contain no impurities at all and therefore have a tendency to order close to the pure T_c. These are called *Griffith singularities* and they are extremely rare and thought to be very weak, and therefore unobservable experimentally.

In the random field systems where the randomness couples to the local order parameter, magnetization, the disordering effect of the random fields wins over and it is much stronger than the thermal fluctuations, which play a secondary role. In the renormalization group calculations the exponent θ_{RF}, which couples to the temperature, is positive and has a negative sign in front of it, $dT = -\theta_{RF}T$. Hence during the renormalization procedure the temperature flows to zero and it is said to be an *irrelevant* parameter,

and therefore much of the equilibrium properties at finite temperatures are reflected by the zero temperature behavior [1, 5, 11]. In this thesis all the calculations are done at $T = 0$. An exact ground state calculation method, Section 1.4, minimizes the energy defined by Hamiltonians, Eqs. (1) and (2). Thus the entropy effects are neglected and instead of the free energy the ground state energy is studied.

In random Ising magnets especially the dynamics differs from the pure case, *e.g.* coarsening is much slower, as the length scale for growing domains depends logarithmically on time instead of a power-law [5, 29, 30]. In experiments also non-equilibrium dynamics plays a dominant role, *e.g.* there is a hysteresis present in the measurements of DAFF, depending on whether the systems are field-cooled or zero-field-cooled [14]. It is hoped that the results of the static studies done here at equilibrium will give some information for the dynamics as well, since the equilibrium cluster structures should be reflected in the dynamics.

1.3 Domain Walls in Random Magnets

Closely related to the ground state structure of a magnet is the structure of domains and domain walls in the magnet. In order to understand the coarsening in the magnet its domain wall behavior needs to be understood.

Let us start by writing the effective continuum Hamiltonian of a domain wall

$$\mathcal{H} = \int \left[\frac{\Gamma}{2} \{\nabla z(\mathbf{x})\}^2 + V_r(\mathbf{x}, z) \right] \mathrm{d}^D\mathbf{x}. \tag{8}$$

The second term in the integrand is the random potential, which has a general form $\langle V_r(\mathbf{x}, z) V_r(\mathbf{x}', z') \rangle \sim \delta(\mathbf{x} - \mathbf{x}') \mathcal{R}(z - z')$. For the random exchange magnets $\mathcal{R}$ is a delta-function, $\mathcal{R}(z - z') \sim \delta(z - z')$, and in the random field case it is linearly dependent on z, $\mathcal{R} \sim (z - z')$. The first term in the integrand creates the elastic part of the energy, which is (together with a neglected linear contribution of a flat wall) proportional to the area of a rough domain wall with a displacement or height z and to the surface tension Γ. Due to the non-zero surface tension the class of models represented by the Hamiltonian (8) are called *elastic manifolds* [31, 32, 33, 34]. Elastic manifolds are generally defined in dimensions $d = (D + n)$, in which d is the total, embedding dimension of the system. A D dimensional domain wall

has an internal coordinate $\mathbf{x}$ and is able to fluctuate in $n = 1$ dimensions defined by the coordinate z. The embedding dimension of the magnet is thus $d = D + 1$. In the case $D = 1$ the object is a *line*, which is able to fluctuate in $n \geq 1$ dimensions. When $n > 1$ $\mathbf{z}$ becomes a vector instead of a scalar. A special case is RB disorder in $(1 + 1)$ dimensions, which besides being the domain wall of a two-dimensional random exchange Ising magnet is also a so called *directed polymer* (DP) [35]. In the case $d = D$ and $n > 0$ the object is called an *elastic medium*.

Examples of Random Manifolds

The elastic manifolds have a large number of different physical realizations. Besides the domain walls, which are $n = 1$ systems, the $D = 1$ lines with $n = 2$ have experimental realizations as flux lines in type II superconductors, where the applied magnetic field penetrates in vortex bundles. In that case the disorder is present in the form of atomic defects (oxygen vacancies in the doped cuprates), grain boundaries, screw dislocations, etc. [31, 36] One famous suggestion for an experimental realization of the $(1+1)$ dimensional directed polymer is rupture lines when tearing paper [37]. Actually it has been claimed that the geometric properties of quasi-static cracks and directed polymers are similar [38, 39], which can be generalized also for higher D dimensional cracks [40]. Elastic media on the other hand have experimental realizations as vortex-lattices in type II superconductors with high-magnetic field, charge density waves, and Wigner crystals [31, 32].

Static Properties of Random Manifolds

Geometric properties of elastic manifolds are usually characterized by spatial fluctuations. For the mean-square fluctuations one has

$$w^2 = \left\langle \left[z(\mathbf{x}) - \overline{z(\mathbf{x})} \right]^2 \right\rangle \sim L^{2\zeta}, \tag{9}$$

where L is the linear size of the system, the brackets $\langle \dots \rangle$ are the disorder-average over a large random ensemble, and ζ is the corresponding *roughness exponent*. Using the Cole-Hopf transformation [41] the $(1 + 1)$ dimensional directed polymer can be mapped to the non-equilibrium problem of kinetic roughening, to the Kardar-Parisi-Zhang (KPZ) equation [42, 43]. In the

KPZ formalism the exponent ζ has been calculated exactly to be $2/3$ in $(1+1)$ dimensions with RB disorder. For higher D dimensional manifolds with $n = 1$ the functional RG calculations give the approximate values $\zeta \simeq 0.208(4-D)$ for RB disorder and $\zeta = (4-D)/3$ for RF disorder [44]. The expression for ζ tells also that the *upper critical dimension* for the elastic manifold is $D_u = 4$. For RB manifolds with varying n and D the exponents have been derived to be $\zeta \simeq [(4-D)/(n+4)]\{1 + (1/4e)2^{-[(n+2)/2]}[(n+2)^2/(n+4)][1-\ldots]\}$ [33]. Here it should be noted that for the thermal roughening of a domain wall in pure magnets the $(1+1)$ dimensional case is equivalent to a random walk (RW) with the corresponding roughness exponent $\zeta = 1/2$. In $(2+1)$ dimensions the thermal roughening is logarithmic, $w^2 \sim \ln(L)$ [45]. Hence the disorder induced roughness is much greater at large length scales and more important than thermal fluctuations.

In the contexts of the surface roughening and fractals, objects which can be defined with Eq. (9) and have an exponent $\zeta < 1$ are said to be *self-affine*. When the exponent $\zeta = 1$, which is the case for $(1+1)$ dimensional RF magnets (only, when $L > L_b$, see Section 4.2), they are *self-similar* or *fractals* [46, 47]. The roughness behavior may be characterized with the height-height correlation function, $G_k(r) = \langle |z(\mathbf{x})z(\mathbf{x}+r)|^k \rangle \sim r^{\alpha_k k}$, too. If the higher moments k of $G_k(r)$ that define α_k vary, such objects are said to be *multi-affine* or *multi-fractals* [48, 49]. The higher moments are dominated by the largest values of the measure, *e.g.* in the case of the surface roughness the higher moments correspond the largest nearest-neighboring height differences of the surface. In the case of *percolation* when considering a random resistor network, the higher moments of the current correspond to the highest currents, which go through the spanning cluster [47]. This current goes through the *singly connected* or *red sites*, since the total current has to go through them, and the corresponding *multi-fractal dimension* defined by the scaling of the highest non-zero moment of current is the fractal dimension of the red sites.

The average mean energy of an elastic manifold scales linearly with the manifold area, $\overline{E} = E_0 L$. The fluctuations of the energy scale as

$$\Delta E = \left\langle \left(E - \overline{E}\right)^2 \right\rangle^{1/2} \sim L^{\theta}. \tag{10}$$

Thus the expansion of the distribution of the energy is $E \sim E_0 L + E_1 L^{\theta} +$ other non-analytic corrections. Huse and Henley [50] derived by expanding the gradient term in the Hamiltonian (8) and by assuming scaling, a hyper-

scaling relation with ζ,

$$\theta = 2\zeta + D - 2. \tag{11}$$

For domain walls θ is always above zero. For lines or polymers with $D = 1$ in $n > 1$ there is still the open question, whether there exists an upper critical dimension n_c at which disorder-induced $\zeta = 1/2$ as for thermal fluctuations, and thus $\theta = 0$. However, it is known that there exists a T_c for $n > 2$ above which the thermal fluctuations dominate, and on the other hand the disorder induced fluctuations dominate always for $n \leq 2$ [51]. Positive θ again couples to the temperature in the renormalization group sense with a negative sign, $dT = -\theta T$, which implies that the temperature is an irrelevant variable and the $T = 0$ fixed point dominates. However, at the randomness dominated pinned phase the temperature is *dangerously irrelevant*, because at $T = 0$ the (free) energy density is singular [3] and there exist many local minima separated by large barriers scaling also with L^θ [44]. This means that in RG calculations the interesting correlation functions cannot be obtained by setting T to zero [52, 53, 54]. This holds for random field magnets, too, and this is the reason, why the early field-theory calculations with the dimensional reduction suggesting $d_l = 3$ for RF magnets failed [44, 1]. The dangerous irrelevance of the temperature modifies the hyper-scaling law used in the Harris criterion, Eq. (7), for the random field magnets to be $2 - \alpha = (d - \theta_{RF})\nu$ [1, 11]. Note that this exponent θ_{RF}, whose value in 3D is unity or greater but not exactly known [11], is not the same as the domain wall energy fluctuation exponent above.

Nevertheless, it has been shown [51] for a directed polymer at finite temperature $T > 0$ that the fluctuations of the entropy $(\Delta S)^2$ and the internal energy $(\Delta E_{int})^2$ scale linearly with the length of the polymer and cancel out each other. Hence there are only the fluctuations of the free energy $(\Delta F)^2$, which scale with the zero temperature energy fluctuation exponent $2\theta = 2/3$.

One should also mention the *replica techniques*, which have been frequently used for calculations in random systems, especially spin glass problems [7], in addition to the renormalization group calculations. Directed polymers have been shown to obey a weakly broken replica symmetry [55], a "baby-spin glass" phenomenon. This means that the replica symmetric solution of a DP is degenerate with the solution with the broken symmetry. There is a broken replica symmetry *e.g.* if a system does not end up in the same

low temperature state, when the cooling is started from different high temperature configurations. The order of the terms in calculating the partition function is important in a broken replica symmetric case. In that case the probability distribution for the replicated states is nontrivial, *i.e.*, also other states than a single one and its mirror case (all the spins are reversed) have a non-zero probability.

Periodicity in Random Manifolds

Elastic manifolds and media can experience periodic potentials. For elastic manifolds, as in the case of domain walls in magnets, an applied periodicity is often due to the underlying lattice structure [56, 57, 34], which in analytic calculations can be added with an extra sinusoidal modulating potential of wavelength λ, $V_p = V_0 \sin(2\pi z/\lambda)$, in the Hamiltonian (8). In the case of $D = 3$ and $n = 1$ there has been a discussion whether there is a first-order or second-order roughening transition at a certain disorder strength below which the domains are flat due to the pinning by the periodic potential. Also there is an open question how the systems reach the asymptotic rough domain wall -limit for $D = 2$ when decreasing the lattice pinning or increasing the systems size [58].

There are elastic media with periodicity, too, called *periodic elastic media* (PEM) where, as in the case of superconductors, one periodicity is due to the rotational invariance of the phase. A second periodicity is induced when flux lines form a lattice at high magnetic fields. Closely related is the random substrate problem, where a $D = 2$ dimensional surface grows on a random substrate on layers of absorbed atoms in $n = 1$ dimensions [59, 60, 61]. This model also serves as a model for the effect of a random field on the XY-model [59, 60]. After a debate it has been agreed that the roughness scales as $w \sim \ln L$ [in contrast to thermal fluctuations in dimensions $(2+1)$, which grow as $w^2 \sim \ln L$]. This phase is called "super-rough" [59, 60, 61, 62, 63, 64, 65]. The substrate roughness is randomly drawn from the interval $d_i \in [0, 1)$ (in lattice units) and i indexes the position in the substrate. Here, the random substrate leads to a periodically repeated disorder seen by an interface lying above the substrate. This arises due to the fact that the first, third, fifth, *i.e.*, odd n_ith "atoms" (and similarly for even n_ith) deposited at the same position on the random substrate see exactly the same disorder around them. The Hamiltonian for such a solid-on-solid model on a random

substrate is

$$\mathcal{H} = \sum_{\langle ij \rangle} f(z_i - z_j), \tag{12}$$

where $z_i = d_i + n_i$ and f is a convex and symmetric function. This corresponds to a case when the RB disorder is repeated with period $\lambda = 2$ along the growth direction, *i.e.*, the potential $V_r(\mathbf{x}, z + 2) = V_r(\mathbf{x}, z)$.

External Field and Susceptibility in Random Manifolds

Interesting phenomena arise especially when an external field is applied to an elastic manifold. In disordered superconductors the external field is due to the current density j, which together with the magnetic field causes a Lorentz-force driving the vortex lines [36]. The external field gives information about the energy landscape of the random system and in experiments one often measures the susceptibility by applying an external field.

In the Hamiltonian (8) the external field adds an extra potential term $V_h \sim h(z)$. Then the Hamiltonian is also applicable to wetting in a three-phase system, where two of the phases are separated by an interface in a random bulk [66, 67, 68, 45]. In that case $h(z)$ is equivalent to the chemical potential, which tries to bind the interface to the wall, and competes with the random potential, in the presence of which the interface tends to wander in the low energy regions of the system. In the case where $V_h \sim hz^\kappa$ and the mean distance of the interface from the inert wall $\overline{z}$ is of the order of the interface transverse fluctuations $\xi_\perp$, there is a power-law relation, from the minimization of Eq. (8), between the distance of the interface and the external field:

$$\overline{z} \sim h^{-1/(\kappa+\tau)} \sim h^{-\psi}. \tag{13}$$

In this thesis $\kappa = 1$ has been used and thus the wetting-exponent becomes $\psi = 1/(1 + \tau)$, *i.e.*,

$$\psi = \frac{\zeta}{2 - \zeta}. \tag{14}$$

Directed polymers have *anomalous* fluctuations resulting from the regions of the random potential with almost degenerate energy minima, which are

separated by large energy barriers [51, 69, 70]. These spatially large-scale low-energy excitations are rare, but dominate the thermodynamic properties and cause large variations in the structural properties at low temperatures. This is also related to the baby spin-glass phenomenon mentioned earlier. Let us consider a polymer, which is fixed at one end. The polymer may have a small energy excitation with a transverse scale Δ ($\simeq l^{\zeta}$, where l is the linear length of the excitation). The energy excitation scales as $\Delta^{\theta/\zeta}$, gives rise to large sample-to-sample variations in the correlation function, and dominates the disorder averages [70]. At low temperatures the polymer is usually locked in a unique state and is separated from the lowest excited state by a free-energy difference, which can be much higher than the temperature. On the other hand the system may have a nearly degenerate state, to which the thermal fluctuations can cause a large-scale "hopping". These nearly degenerate states are typically separated by large energy barriers and with large distances from the ground state. For the finite field case there is a *statistical tilt symmetry*, which means that the random part of the new potential of the polymer is statistically the same as the old one, when the polymer is excited by an applied field. It has been also shown numerically that the energy difference between two copies of the polymer in the same realization of the random potential scales as L^{θ}, where $\theta = 2\zeta - 1 = 1/3$ [69]. When a polymer is fixed at one end and an external field h is applied to the other end of the polymer, the polymer does sharp jumps of distance L^{ζ}, when the field is increased by L^{θ}. Calculating the susceptibility, $\chi \sim \langle z^2 \rangle - \langle z \rangle^2$, in this case leads typically $\chi/L = 0$, *i.e.*, it is stationary for large ranges of applied field. With the probability $L^{-\theta}$ there is a sample for which $h = 0$ is the critical value of h, and the polymer makes a large jump of height $L^{2\zeta} \sim L^{1+\theta}$. Hence the total average susceptibility becomes $\chi_{ave} \sim L$.

The response of the random manifolds to the external field is seen in their susceptibility. In this thesis the susceptibility used for a D dimensional manifold in a d dimensional embedding is [71]

$$\chi = \lim_{h \to 0+} \left\langle \frac{\partial m}{\partial h} \right\rangle , \tag{15}$$

where the change in the magnetization of the whole d dimensional system is calculated in the limit of the vanishing external field, which is applied to the whole system, from the positive side. Note that the manifold is not fixed at any point. This definition is used instead of the one used in

the studies with the field applied in the end point of the polymer, since it is more practical for higher dimensional manifolds and corresponds to the case the extra field potential $V_h \sim hz$ is added in the Hamiltonian (8). It should be noted that the magnetization of the system with a domain wall $m \equiv 2\left[1 - z(\mathbf{x})/L_z\right] - 1$, where L_z is the system height in the direction of the average normal vector of the manifold.

1.4 Computing Exact Ground States

Calculating random systems using conventional Monte Carlo methods usually leads to problems, since due to the rugged energy landscape and deep metastable energy minima, which are separated by high barriers, finding the true global energy minimum and equilibrium state is difficult and slow. Finding the ground state structure is actually a *global optimization problem.*

In this thesis for the numerical studies of the Hamiltonians, Eqs. (1) and (2), the spin-systems are transformed to random flow graphs. When the manifolds are considered, these systems have domain wall -enforcing boundary conditions, such that the spins in the opposite boundaries are fixed to point up and down and the domain wall is the path between the up and down spin domains which is formed when the energy is minimized. The transformation is such that there are two extra sites in the graph: the source (s) and the sink (t), and the coupling constants $2J_{ij} \equiv c_{ij}$ between the spins correspond to flow capacities $c_{ij} \equiv c_{ji}$ from a site S_i to its neighboring one S_j. In the random field systems the positive field values $2h_i$ correspond to flow capacities c_{it}, $c_{it} \equiv c_{ti}$ connected to the sink from a spin S_i, similarly the negative fields with c_{is} are connected to the source, see a sketch in Fig. 2. For domain walls in random exchange magnets the sink is formed by the spins, which are forced to be up and the source is formed by the spins, which are forced to be down, see Fig. 1.

From these random graphs using a graph-theoretical combinatorial optimization algorithm, a *maximum-flow minimum-cut algorithm*, the bottleneck, which restricts the amount of the flow that is able to flow from the source to the sink, can be found exactly [72, 73]. This bottleneck, path P, divides the system in two parts, sites connected to the sink and sites connected to the source. It is the global minimum cut of the graph. The sum of the capacities, *i.e.*, the unsatisfied coupling constants and fields, belonging to the cut equals the maximum flow. The minimum cut is smaller than

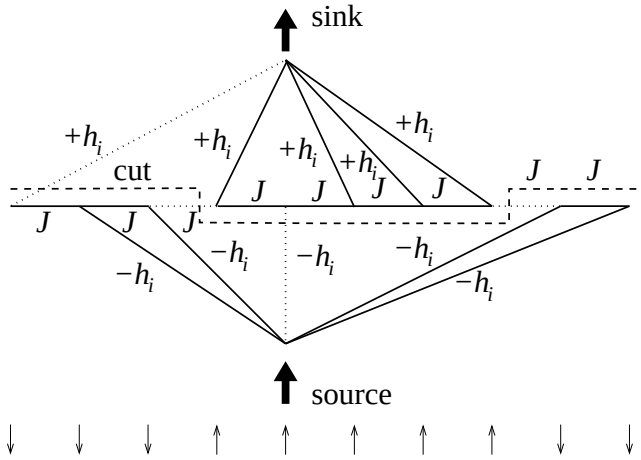

Figure 2: A random graph for calculation of a one-dimensional random field magnet. The dotted lines represent unsatisfied capacities, *i.e.*, fields or bonds, and the solid lines represent the satisfied ones. The maximum flow is pushed from the source to the sink, and the minimum cut, drawn with a dashed line, defines the ground state. Its spin-structure is plotted in bottom of the figure.

of any other path cutting the system, and it gives either the ground state structure of a random field magnet with or without a domain wall, or the domain wall structure for the random exchange magnet. The value of the maximum flow is

$$\mathcal{F} = \sum_P c_{ij} + \sum_P c_{it} + \sum_P c_{is}, \tag{16}$$

where the sums are over the capacities belonging to the minimum cut. The last two terms are not needed for the random exchange magnets. The total energy is achieved by adding in the Hamiltonians (1) and (2) the values defined by (16). For the random exchange magnet (here $S_i = 1$)

$$\mathcal{H} = -\sum_{\langle ij \rangle} J_{ij} + 2 \sum_{unsat.} J_{ij} = -\sum_{\langle ij \rangle} J_{ij} + \sum_P c_{ij}, \tag{17}$$

where $\langle ij \rangle$ is over *all* (satisfied and unsatisfied) nearest-neighbor pairs, and for the random field magnet

$$\begin{aligned} \mathcal{H} &= -\sum_{\langle ij \rangle} J_{ij} - \sum_i h_i + 2 \sum_{unsat.} J_{ij} + 2 \sum_{unsat.} h_i \\ &= -\sum_{\langle ij \rangle} J_{ij} - \sum_i h_i + \sum_P c_{ij} + \sum_P c_{it} + \sum_P c_{is}. \end{aligned} \tag{18}$$

Thus the optimized maximum flow gives the smallest value which increases the energy from a large negative value. Note, however, that in the calculations done in this thesis the reported energy values are actually the maximum flow values $\mathcal{F}$. The first terms in Eqs. (17) and (18) are statistically constant for a fixed system size and strength of randomness, and thus may be set to zero. The maximum flow algorithms can be proven to give the exact minimum cut of all random graphs, in which the capacities are non-negative and where there is a single source and sink [74]. In physical situations this means systems without local frustration, and thus *e.g.* spin-glasses or Potts models cannot be studied with them. However, DAFFs can be studied by doing a standard mapping to a random field magnet.

The idea to use the maximum flow method in order to calculate ground states in random field Ising magnets was introduced in mid-eighties [75, 76]. The algorithm was used for the first time in this context in '86 to show that the 3D RFIM has a ferromagnetic phase [77]. The best known maximum flow method is by Ford and Fulkerson and is called the *augmenting path method* [78]. In this thesis a more sophisticated method called *push-and-relabel* by Goldberg and Tarjan is used [79]. The algorithm is optimized for the calculations done here and the details of the implementation of the algorithm have been reported already in a Master's Thesis [80]. The algorithm scales almost linearly, $\mathcal{O}(n^{1.2})$, with the number of spins and gives the ground state for a million spins in about one minute in a workstation.

When one wants to study the response to a perturbation, *e.g.* an external field, a technique, which takes advantage of the so called *residual* graph can be used [81]. In this thesis the technique is used for calculating so called *red clusters*, see Section 4.4 and Publication VII. In the algorithm the original ground state is searched without a perturbation. Then the perturbation is applied, and the ground state is searched again. This time all the flow needs not to be constructed from scratch, but instead one can utilize the final situation of the first ground state search (the residual graph). Only the extra amount of flow by which the perturbation is done has to be forced to flow through the system from the source to the sink.

It should be mentioned, too, that for the $(1+1)$ dimensional domain walls there is another efficient method available, the so called *transfer matrix method* [82]. In the maximum flow method domain walls may include *overhangs*, in the transfer matrix method usually not.

1.5 Rare Events and Extreme Statistics

Many of the interesting phenomena studied in this thesis relate to *extreme statistics* [83]. These are *e.g.* the destruction of the effective ferromagnetic phase in two-dimensional random field magnets, when the system size increases, Section 4.1, the roughening of the elastic manifolds, Section 2.2, and the response of an elastic manifold to an external field, Section 3.1, or to an applied potential, Section 2.2, etc.

Extreme statistics is found in several fields. Extreme values are the smallest or the largest ones of statistically distributed measures, such as the first failure of an equipment; service time of an equipment, when it is determined by the component, which requires the longest service; and the breaking strength of a material, etc. The basic idea is to have independent and identically distributed random variables and to study either tail of the distribution, and how these extreme values themselves are distributed [83]. The extreme statistics naturally depends on the original distribution, from which the independent and identically distributed random variables are taken.

Let us have random values, *e.g.* of energy, which are taken from a distribution decaying faster than any power-law,

$$\mathcal{P}(E) = k \exp\left\{ - \left(\frac{|E - \langle E \rangle|}{\Delta E} \right)^{\eta} \right\}, \tag{19}$$

where $\eta > 0$ [84], and $\langle E \rangle$ is the average energy of the system and $k \sim (\Delta E)^{-1}$ normalizes the distribution. The case $\eta = 2$ is a Gaussian distribution. Approximating a distribution with the Gaussian one holds for the field energy of the two-dimensional random field magnets, when observing the appearance of the first domain, since the random fields are by definition from Poissonian statistics. The Gaussian approximation holds also for the flat domain wall energy when the wall roughens. For the rough domain walls, the exponent η may change due to their global optimization character. For example for $(1 + 1)$ dimensional directed polymers, η is known to vary [85, 35]: the bulk of the distribution of the energy of a directed polymer is Gaussian, and for the tails, for $E < E_{min}$ and $E > E_{max}$, $\eta_- = 1.6$ and $\eta_+ = 2.4$, respectively. For higher dimensional manifolds the shape of the distribution is not known in detail [52].

Assuming a priori that there are N local minima in a system, we get the

probability of the lowest energy to be E

$$L_N(E) = N\mathcal{P}(E)\left\{1 - C_1(E)\right\}^{N-1}. \tag{20}$$

where $C_1(E) = \int_{-\infty}^{E} \mathcal{P}(e)\, de$ is called the error-function when $\eta = 2$. In the case $\mathcal{P}(E)$ is Gaussian likewise for a general $\eta > 0$, $L_N(E)$ is known to be Gumbel distributed, $\exp(u - \exp u)$ [84, 86, 87]. In the cases studied here $L_N(E)$ is not trivially Gumbel distributed, since the original distributions have cut-offs, due to the fact that the energy has to have a nonzero value.

The average of the lowest energy is given by

$$\langle E_0 \rangle = \int_{-\infty}^{\infty} E L_N(E)\, dE, \tag{21}$$

and the typical value of the lowest energy is estimated from

$$N\frac{1}{k}\mathcal{P}(\langle E_0 \rangle) \approx 1. \tag{22}$$

Note, that in approximating the integral, Eq. (21), with the aid of the distribution, Eq. (22) [in the limit $C_1(E)$ in Eq. (20) is small], the normalization $1/k$ should be taken into account. Eq. (22) gives

$$\langle E_0 \rangle \sim \langle E \rangle - \Delta E \left[\ln N\right]^{1/\eta}. \tag{23}$$

Similarly one may proceed, *e.g.* in studying the average *gap* between the lowest and the next lowest energies, see Sections 2.2 and 3.2 and Publications II, IV, and V.

2 Elastic Manifolds with Periodicity

In this Section two types of periodic elastic manifolds are studied. The results of the work done are published and explained in more detail in articles I and II. The first type of periodicity is periodic elastic media, where the random potential is repeated. The second type of periodicity is achieved by adding an extra modulating potential.

2.1 Periodic Elastic Media

In Publication I it is shown that an elastic manifold defined by the Hamiltonian (8), where the randomness is periodically repeated with a period of λ, *i.e.*, $V_r(\mathbf{x}, z + \lambda) = V_r(\mathbf{x}, z)$, leads to the random substrate problem, Eq. (12), whenever the period is finite. This is seen when the system size is increased, and thus when approaching the thermodynamic limit, as a crossover from the random manifold roughness exponent to the periodic elastic media roughness exponent.

The exact ground state calculations are done for $(1+1)$ and $(2+1)$ dimensional systems with random-bond disorder by varying the periodicity λ and the system size L. The average normals of the interfaces lie in the $\{10\}$ or $\{11\}$ directions of square lattices and in the $\{100\}$ or $\{111\}$ directions of cubic lattices, respectively.

There are two limits for the periodicity: $\lambda = 2$ and $\lambda = \infty$. The first case corresponds to the periodic elastic media and the second to the random bond manifold. In $(1 + 1)$ dimensions when $\lambda = 2$, the manifold has only two choices, whether to go up or down. This is the same question which a random walker makes, and thus the roughness exponent becomes $\zeta = 1/2$. When $\lambda = \infty$ the manifold is actually a directed polymer, *i.e.*, it has a greater exponent from global optimization $\zeta = 2/3$. Similarly in $(2 + 1)$ dimensions for $\lambda = 2$, $w \sim \ln L$ as was stated in Section 1.3 and for $\lambda = \infty$, $\zeta = 0.41 \pm 0.01$.

The scaling functions for roughness with different λ and L are derived. In $(1 + 1)$ dimensions:

$$w(L, \lambda) \sim L^{2/3} f\left(\frac{L}{\lambda^{3/2}}\right), \tag{24}$$

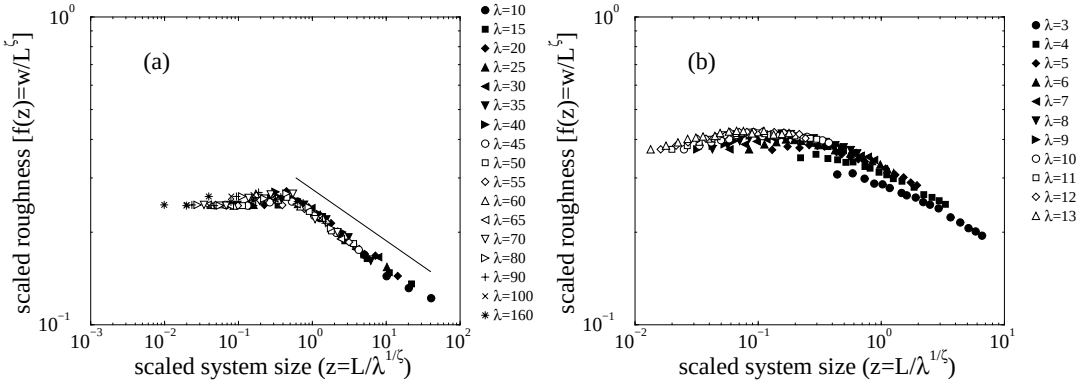

Figure 3: (a) The scaling function $f(z) = w/L^{\zeta}$ for two-dimensional systems of the roughness $w(L, \lambda)$ vs. scaling parameter $z = L/\lambda^{1/\zeta}$, where $\zeta = \zeta_{DP} = 2/3$. The solid line has a slope of $\zeta_{RW} - \zeta_{DP} = -1/6$. (b) The scaling function $f(z) = w/L^{\zeta}$ for three-dimensional systems of the roughness $w(L, \lambda)$ vs. scaling parameter $z = L/\lambda^{1/\zeta}$, where $\zeta = 0.42$.

where the scaling function $f(z)$ for the roughness has the asymptotic behavior

$$f(z) \sim \begin{cases} \text{const} & z \ll 1, \\ z^{-1/6} & z \gg 1, \end{cases} \tag{25}$$

see Fig. 3(a). Similarly in $(2+1)$ dimensions:

$$w(L, \lambda) \sim L^{\zeta_{RB}} f\left(\frac{L}{\lambda^{1/\zeta_{RB}}}\right), \tag{26}$$

and the scaling function is

$$f(z) \sim \begin{cases} \text{const} & z \ll 1, \\ \ln z / z^{\zeta_{RB}} & z \gg 1, \end{cases} \tag{27}$$

see Fig. 3(b).

2.2 Elastic Manifolds with an Additional Periodic Potential

Elastic manifolds with an extra applied potential and random bond disorder are always in $(1+1)$ and $(2+1)$ dimensions in the random-bond universality class regardless of the applied potential. However, there are two types

of *intermittence* seen before the asymptotic roughness behaviors with exponents $\zeta = 2/3$ and $\zeta = 0.41 \pm 0.01$ in $(1+1)$ and $(2+1)$ dimensions, respectively. The first intermittence is due to large fluctuations between different potential valleys of the mean location of a flat manifold, and the second type of intermittence happens when the manifold roughens over the potential barriers, see Publication II.

The calculations are done for systems with random bond disorder having an extra potential $V_p = V_0[0.5\sin(2\pi z/\lambda) + 0.5]$ in Hamiltonian (8) for $\{11\}$ and $\{111\}$ oriented lattices. The essential tuning parameter is $v = V_0\lambda J/\delta J$, where the average value of the exchange constant is $J = 1$ and the uniform distribution of random bonds has a width δJ, and λ is the wavelength of the potential. For large values of v the interface is always pinned near a minimum of the periodic potential, but it jumps between different minima as v is varied. See an example in Fig. 4(a) for $(1+1)$-dimensional case with various V_0 and a fixed random configuration.

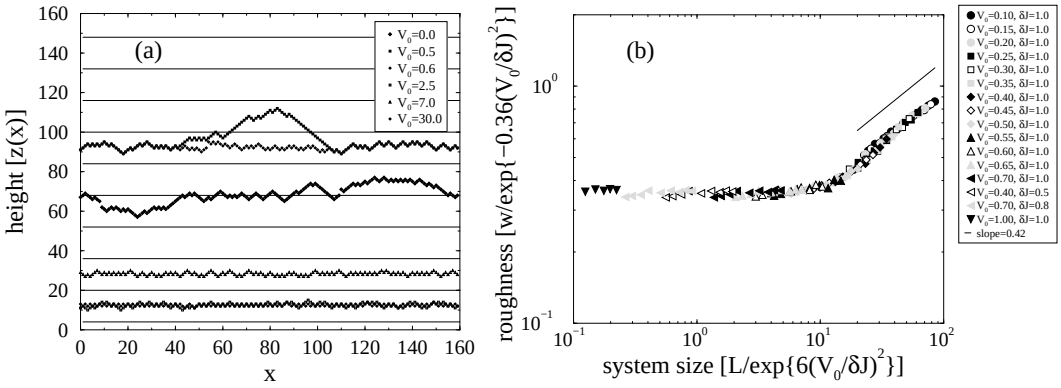

Figure 4: (a) Interface configurations in $(1+1)$-dimensions for various V_0. The disorder configuration and wavelength ($\lambda = 16$) are fixed at $\delta J = 1$, and the disorder is *exactly* the same for each value of V_0. The solid lines denote the position of the largest values of the sinusoidal periodic potential V_p. Interfaces are oriented along the $\{11\}$ direction. (b) Scaled roughness of interfaces oriented in $\{111\}$ directions for various values of $V_0/\delta J$ and L. $\lambda = 4$. The solid line corresponds to the slope $\zeta = 0.42$.

Using an extreme statistics argument, Section 1.5, the gap between the energies of the manifolds, pinned in the periodic potential minima having the lowest energy and the next lowest energy, is derived. This gap energy is compared with the variations of the energy, when the manifold is pinned in the minimum, resulting from the variations of the amplitude of the periodic

potential. Balancing these two energies it is approximated that the number of the minima the manifold visits when v is swept is $\ln(N)/\{\ln(L^{d-1})\}^2$ of the N available minima of the potential. Similar chaos behavior can be seen for a directed polymer, when adding a random perturbation to the system [88, 89].

When v is decreased even more, the manifolds start to roughen and wander over the pinning barriers, see the two smallest V_0 in Fig. 4(a). Using an Imry-Ma type of argument [4] (see Section 1.2) and the extreme statistics estimation, the length scale at which a $(2+1)$ dimensional manifold roughens,

$$L_1 \sim \exp\left[\left(\frac{V_0\lambda}{\delta J}\right)^2\right], \tag{28}$$

is calculated. It is shown in Publication II that on the average the first droplet, which goes over the energy barrier of the periodic potential, is half of the manifold size, and thus leads to a first-order type of a cross-over in roughness. This result should have some relevance to the debate presented in Section 1.3 [58].

Using the cross-over length scale, L_1, the roughness data with various values of $V_0/\delta J$ and L can be collapsed, see Fig. 4(b) for $(2+1)$ dimensional case. In the asymptotic limit, for $L > L_1$, the random manifold roughness exponents, $\zeta = 2/3$ in (1+1) dimensions (Publication II) and $\zeta = 0.41 \pm 0.01$ in $(2+1)$ dimensions, are reached.

For {100} oriented lattices without an applied potential similar scaling behavior is seen. In this case the extra potential gets introduced due to the lattice itself. The same cross-over length L_1, Eq. (28), holds for the roughening transition here, too (Publication II). This differs from the earlier result of a study where the amplitude $A(p)$ of the roughness behavior $w \sim A(p)L^{\zeta}$ has been investigated [90]. The amplitude has a linear behavior with respect to the strength of the dilution type of disorder, *i.e.*, the probability of undiluted bonds p. By extrapolating from the linear behavior, a critical $p_* \simeq 0.89 \pm 0.01$ was derived, above which the amplitude seems to have a value zero. However, the scaling behavior confirmed in this thesis indicates that the roughening cross-over happens at such large length scales for p close to unity, that it cannot be seen for the finite system sizes used in the study [90], and $A(p)$ is non-linear for $p > p_*$.

3 Elastic Manifolds in an External Field

The response of elastic manifolds or interfaces to the external field is studied in this Section. The results are reported in detail in Publications III–V. First, based on an energy landscape argument the movement of a manifold at equilibrium, when an external field is applied, is studied, Section 3.1. The susceptibility of the manifold is derived in Section 3.2 from the probability distribution of the field, when the manifold experience its first *jump*, and from the finite size scaling of the *first jump field*. To finish the story of the external field response of elastic manifolds the random-bulk wetting phenomenon is considered in Section 3.3.

3.1 Glassy Energy Landscapes

The elastic manifolds are studied in dimensions $(1+1)$ and $(2+1)$ with random-bond disorder in $\{10\}$ and $\{100\}$ oriented lattices, with an extra potential caused by a field $V_h \sim hz$ in the interface Hamiltonian (8). The field is actually added to exchange constants so that $J_\perp(z) = J_{random} + h(z)$, where $J_\perp$ are couplings in the z-direction, the direction of the average normal vector of the manifold. When a ferromagnetic system is studied, the external field $h(z)$ can be transformed to a constant external field term $-H\sum_i S_i$ in the bulk Hamiltonian (2) with fixed boundaries.

Based on the anomalous fluctuations of directed polymers, Section 1.3, the external field contribution to a manifold is generalized. Let us consider a manifold, which is fixed in one end, then the next optimal position of the manifold has a displacement Δ from the original state to the z direction and the displacement scales as $\Delta \sim L^\zeta$. If on the other hand the energy *gap* between two manifolds with energies E_0 and E_1 grows as $E_1 - E_0 \sim L^\theta$, then it follows that $E_1 - E_0 \sim \Delta^{\theta/\zeta}$. The external field has a contribution for the energy differences of interfaces $E_1 - E_0 \sim hL^D\Delta \sim h\Delta^{1+D/\zeta}$. Assuming that this difference balances the gap and using the hyper-scaling law $\theta = 2\zeta + D - 2$ it leads to

$$h \sim \Delta^{\overline{\alpha}} = \Delta^{(\zeta-2)/\zeta}. \tag{29}$$

The exponent $\overline{\alpha}$ is negative assuming that the roughness exponent is below two, which is satisfied for both types of disorders studied in this thesis. Hence, smaller fields scale with larger excitations and thus large excitations

are the preferred ones, at least below the upper critical dimension. Eq. (29) works only for ferromagnetic RF systems. If the bulk of a RF magnet is paramagnetic the interface stiffness vanishes and $\Delta E = E_1 - E_0$ does not scale. The scaling argument (29) is for an average or a typical behavior, but here we are interested in the smallest field excitations, *i.e.*, in an extreme behavior, and thus the scaling argument has to be checked for them. In Publication V we have calculated for directed polymers, which are not fixed at any point, the fraction of the first excitations for which the next optimal position has an overlap with the original position. This overlap versus the system size has a power-law behavior with a negative exponent. Hence in the thermodynamic limit the excitations are always without an overlap between the original and the next state.

In Fig. 5(a) it is shown what happens for two different random realizations of DPs, when a perturbing external field is applied: the mean height of the polymer normalized by its original height $\overline{z}/\overline{z}_0$ is shown, when the external field is increased. For both cases there is a large *jump* of a size about half of the height of DP's original position at *first jump field*, which is $h_1 = 8 \times 10^{-5}$ (case 1°). As a finite size effect the case 2° is preceded by a smaller jump. This leads to a picture in which assuming a starting position far enough from the system boundary, a finite number of large jumps exists from the original position $z_0(\mathbf{x})$ to the positions $z_1(\mathbf{x}), \ldots, z_n(\mathbf{x}), \ldots$, closer and closer to the wall, *i.e.*, $z_0(\mathbf{x}) > z_1(\mathbf{x}) > \ldots > z_n(\mathbf{x}) > 0$.

The global changes (large jumps) induce finite changes in the magnetization m, and are reminiscent of first-order phase transitions and level-crossings between the valleys in the energy landscape for the interface. The idea of level-crossing is sketched in Fig. 5(b). In order to change between the geometrically separated minima, an external field is applied, which at jumps plays the role of latent heat. Originally the interface lies at height $\overline{z}_0$ and has an energy E_0. When the field is applied interface's energy increases by $hL^D\overline{z}_0$ and at h_1 the interface jumps to $\overline{z}_1 < \overline{z}_0$ having energy $E(h_1) = E_1 + h_1 L^D \overline{z}_1 = E_0 + h_1 L^D \overline{z}_0$, where E_1 is the energy of the interface at z_1 without the field. A similar behavior takes place at h_n, $n = 2, 3, \ldots$, when the interface moves from $\overline{z}_{n-1}$ to $\overline{z}_n < \overline{z}_{n-1}$.

We have assumed that the roughness exponent ζ does not define only the width of the manifold, but also the width of the minimum energy valley, *i.e.*, L^ζ is the only relevant length scale in the transverse direction, and thus the manifold should have $N_z \sim L_z/L^\zeta$ minima from which to choose the global minimum position. For $\zeta < 1$ the number of the minima grows with

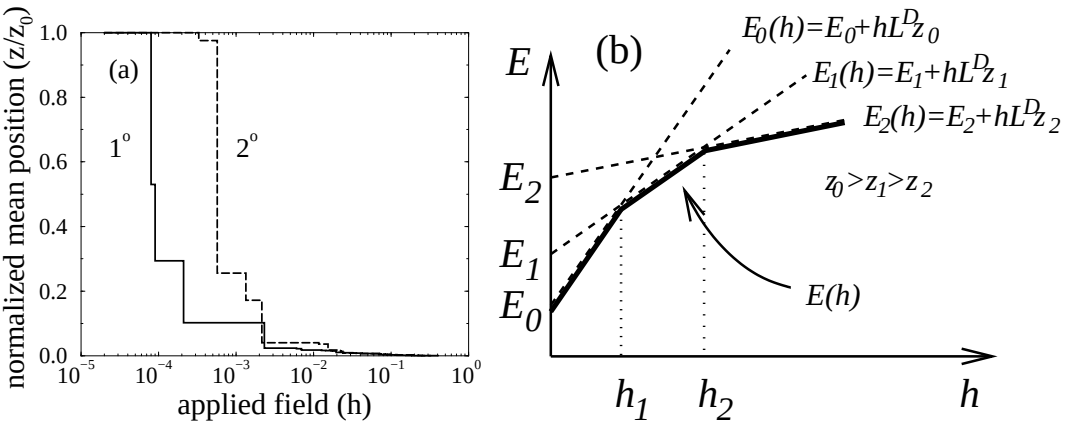

Figure 5: (a) Examples of two realizations of changes in mean heights $\bar{z}$ of interfaces normalized by their original (global minimum) positions $\bar{z}_0$ vs. applied field h for (1+1) dimensional systems. Note the large jumps in both cases. (b) The level-crossing phenomenon for interfaces in random systems in the presence of an external field.

system size, if the geometry is kept isomorphic, $L_z \propto L$. The requirement $\zeta < 1$ holds for all RB interfaces; and for ferromagnetic RF interfaces, when $D > 1$.

Following similar arguments as in deriving Eq. (29) for an excitation, the mean field result for the finite size scaling of the first jump field is derived. Let us have an interface at an arbitrary height z_0 with an energy E_0 and an isotropic system $L \propto L_z$. The energy gap between the two lowest energy minima scales as $\Delta E_1 \sim L^\theta$. On the other hand the energy difference of elastic manifolds at different heights due to the field contribution is $\Delta E \simeq h\Delta z L^D$. Assuming that $\langle \Delta z \rangle \sim L_z$ the field contribution becomes $\Delta E \sim hL^d$. It is expected that the first jump happens, when the gap equals the field energy, and thus the first jump field scales as

$$\langle h_1 \rangle \sim L^\alpha = L^{\theta - d}. \tag{30}$$

In Publications III and V the scaling, Eq. (30), and the assumption $\langle \Delta z \rangle \sim L_z$ are confirmed numerically for directed polymers and in Publication V for $(2+1)$ dimensional random-bond manifolds.

3.2 Susceptibility of Domain Walls

The susceptibility of domain walls is studied here based on the probability distribution of the first jump field and the energy gaps, and on their finite size scaling.

All the energy minima are assumed to be non-correlated and well separated from each other, see Fig. 6(a). This picture can be compared with the idea of hierarchical parabolic wells of random depth used in functional RG and replica calculations for elastic manifolds [91]. In Fig. 6(a) we have a global energy minimum E_0 at z_0, and energy gaps $\Delta E_1 = E_1 - E_0$ and $\Delta E_{1^*} = E_{1^*} - E_0 > \Delta E_1$ with energies E_1 at z_1 and E_{1^*} at z_{1^*}, respectively. Note, that here the energy values as well as the field contributions are normalized by L^D which is constant when the system size is fixed. Then the field h is applied, *i.e.*, the energy landscape is tilted, see Fig. 6(b). Due to the statistical tilt symmetry the external field h is assumed not to change the shape of the random landscape. At the smallest tilt so that the interface moves, *i.e.*, at field h_1, it moves to z_{1^*}, since with the field h_1 $E_0(h_1) = E_0 + h_1 z_0 = E_{1^*}(h_1) = E_{1^*} + h_1 z_{1^*} < E_1(h_1) = E_1 + h_1 z_1$.

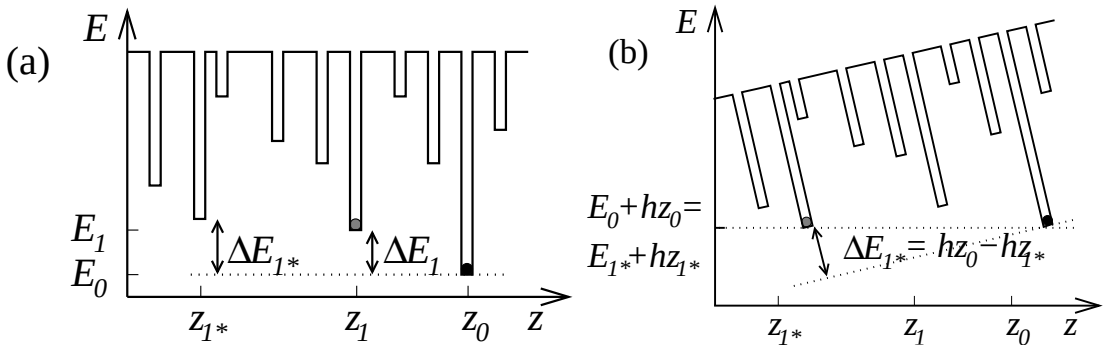

Figure 6: (a) A simplified view of the minima in the energy landscape of a random system. $\Delta E_1 = E_1 - E_0$ is the energy gap between the ground state at z_0, denoted with a black circle, and the second lowest minimum at z_1 denoted with a gray circle. (b) The view of the minima in the random system when the field is applied.

Using a probabilistic argument the probability distribution of the first jump

field h_1 becomes

$$P(h_1) = \exp\left[-\int_1^{N_z}\int_0^{kh_1/N_z} \hat{P}(\Delta E)\, d(\Delta E)\, dk\right] \times \int_1^{N_z} \frac{\hat{P}(kh_1/N_z)}{1-\int_0^{kh_1/N_z} \hat{P}(\Delta E)\, d(\Delta E)}\, dk, \tag{31}$$

where $\hat{P}(\Delta E)$ is the probability distribution of the gap energies. For a more complete derivation, see Publication V.

Approximating $\hat{P}(\Delta E_1)$ with a uniform distribution (in Publication V various distributions are discussed) the probability distribution of the first jump field is derived to be

$$P(h_1) = \exp\left[-\frac{N_z h_1}{2}\right] \frac{N_z}{h_1} \ln\left[\frac{1-\frac{h_1}{N_z}}{1-h_1}\right] \sim \exp(-h_1), \tag{32}$$

see Fig. 7(a) for a (1+1) dimensional case. It should be noted that the distribution from the numerical calculations is wider than the exponential line, Eq. (32), in the figure. The normalization of the distribution leads to the fact that the numerical result lies below the exponential line at $P(h_1 \simeq 0)$, as well.

Following an extreme statistics argument as in Section 1.5 for the lowest average energy $\langle E_0 \rangle$ of a manifold from a system with $N_z \sim L_z/L^{\zeta}$ energy minima we get

$$\langle E_0 \rangle \sim \langle E \rangle - \Delta E \left[\ln(N_z)\right]^{1/\eta}, \tag{33}$$

and similarly for the gap energy $\langle \Delta E_1 \rangle$

$$\langle \Delta E_1 \rangle \approx \frac{\Delta E^{\eta}}{\eta(\langle E \rangle - \langle E_0 \rangle)^{\eta-1}} \approx \frac{\Delta E}{\eta \left[\ln(N_z)\right]^{(\eta-1)/\eta}}. \tag{34}$$

The detailed derivation is reported in Publications IV and V.

In order to derive the scaling function for ΔE_1 it is expected that in systems, where height L_z is small enough to restrict the number of minima, ΔE_1 mainly depends on the height of the system L_z. On the other hand, when L_z is large enough, there are enough valleys from which to choose the two minima, and one has $\Delta E_1 \sim \Delta E \sim L^{\theta}$, hence

$$\langle \Delta E_1(L, L_z) \rangle \sim \begin{cases} \tilde{f}(L_z), & L_z \ll L, \\ L^{\theta}, & L_z \gg L. \end{cases} \tag{35}$$

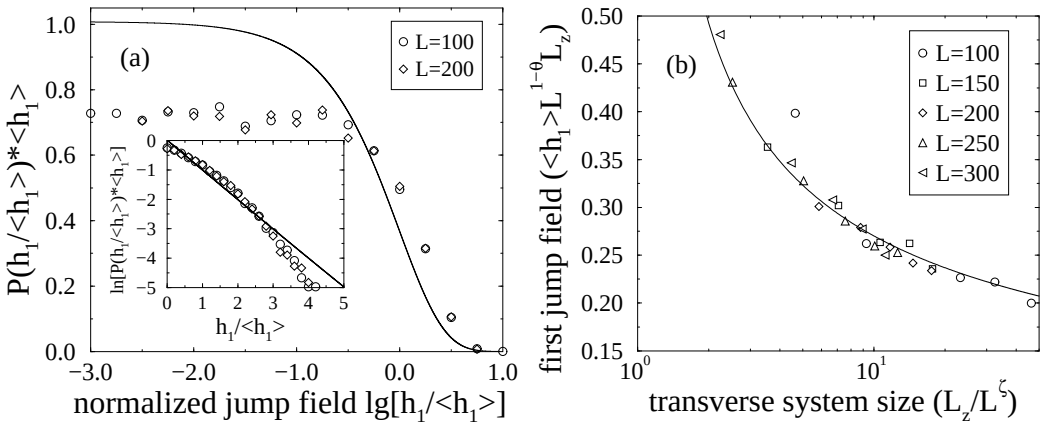

Figure 7: (a) The scaling function of the probability distribution $P(h_1/\langle h_1\rangle) \times \langle h_1\rangle$ for the first jump field values h_1 normalized by their disorder-average $\langle h_1\rangle$. The inset shows the tails in the natural-log-scale. The initial global minimum position $\bar{z}_0/L_z \simeq$ const for both L. The line is the analytic result from Eq. (32). (b) The scaling function $f(y)$ of the scaled disorder-average of the jump field $\langle h_1\rangle L^{1-\theta}L_z$ as a function of scaled transverse system size L_z/L^{ζ}. The line $f(y) = 0.41\ln(y)^{-1/2}$ is a guide to the eye. Also here $\bar{z}_0/L_z \simeq$ const.

Since it is assumed that $L_z \sim L^{\zeta}$, a natural scaling form based on these limiting behaviors is

$$\langle \Delta E_1(L, L_z)\rangle \sim L^{\theta} f\left(\frac{L_z}{L^{\zeta}}\right). \tag{36}$$

The argument $y = L_z/L^{\zeta}$ for the scaling function $f(y)$ is just a function of the number of the minima, *i.e.*, $L_z/L^{\zeta} \sim N_z$, and the scaling function has the form from Eq. (34), when $\eta = 2$, (see Section 1.5 for discussion of η)

$$f(y) \sim [\ln y]^{-1/2}. \tag{37}$$

Publications IV and V include the numerical data confirming the scaling.

In order to find the scaling relation for the first jump field h_1, an Ansatz $\langle \Delta E_1\rangle = \langle h_1\rangle L L_z$ is made, since the field contributes to the manifold energy proportional to L^D (here $D = 1$) and $L_z \sim \langle \Delta z_1\rangle$ is the difference in the field contributions hz to the energy at finite h at different average valley heights z_0, z_1. Hence

$$\langle h_1(L, L_z)\rangle L L_z \sim L^{\theta} f\left(\frac{L_z}{L^{\zeta}}\right), \tag{38}$$

where the scaling function $f(y)$ for the number of the minima $N_z \sim L_z/L^\zeta \sim y$ has the scaling function Eq. (37). Fig. 7(b) shows the scaling function (38) with a collapse of $\langle h_1(L, L_z)\rangle L^{1-\theta} L_z$ versus L_z/L^ζ for various L and L_z in $(1 + 1)$ dimensions with a good agreement. Generalizing the numerical results of $(1+1)$ and $(2+1)$ (the numerical data for the latter case is shown in Publication V) dimensional calculations to arbitrary dimensions give the behavior of $\langle h_1(L, L_z)\rangle \sim L^{\theta-D} L_z^{-1} [\ln(L_z/L^\zeta)]^{-1/2}$.

The susceptibility per spin of a system with a domain wall, Eq. (15) in Section 1.3, may be written in the form

$$\chi = \lim_{h\to 0+} \left\langle \frac{\Delta m(h)}{\Delta h} \right\rangle \simeq \left\langle \frac{\Delta z_1}{L_z} \right\rangle \lim_{h\to 0+} P(h_1), \tag{39}$$

where $P(h_1)$ is the probability distribution of the first jump fields with the corresponding first jump size Δz_1, and the magnetization $|m(h)| \sim z(h)/L_z$. The limit $h \to 0+$ is taken from the probability of having a jump, and thus the susceptibility will reflect the "co-existence" phenomenon related to the first-order transition. Since $\langle \Delta z_1 \rangle \sim L_z$, the finite size scaling of the susceptibility per spin depends only on the probability distribution of the first jump field at the limit of the vanishing external field. The probability distribution has a finite value at $P(h_1 = 0)$, see Fig. 7(a), and $\langle h_1(L, L_z)\rangle$ vanishes with increasing system size, and thus from the normalization factor at $P(h_1 = 0)$ the scaling of the susceptibility becomes

$$\chi \sim L^{D-\theta} L_z [\ln(L_z/L^\zeta)]^{1/2}, \tag{40}$$

and at the isotropic limit, $L \propto L_z$, the total susceptibility $\chi_{tot} = L^d \chi$ is

$$\chi_{tot} \sim L^{2D+1-\theta} [(1 - \zeta) \ln(L)]^{1/2}. \tag{41}$$

This differs from an earlier result [71], where assuming smooth, analytic behavior in the manifolds' thermodynamic functions, the susceptibility (for a surface of dimension D) being proportional to the displacement of the manifold was derived to be $\chi_D \sim L^{D+2}$ and the susceptibility per unit hyper-surface to vary as L^2 for a manifold of scale L. This result was found to be independent of the type of the pinning randomness, too. The studies here take into account the anomalous fluctuations of the manifolds and scaling of the number of the energy minima, which lead to a logarithmic factor in the susceptibility. It should be noted that the formula for the susceptibility in Publication III lacks this logarithmic factor. The correct formula is reported in Publications IV and V.

3.3 Random-Bulk Wetting

In order to see the wetting behavior, let us study the case $L_z \ll L$, so that there is only one valley available, and the assumption that the interface is near a wall holds for the wetting behavior, see Section 1.3. In Fig. 8(a) the average mean heights $\langle \overline{z}(h) \rangle$ versus the field h for $(1+1)$ and $(2+1)$ dimensional manifolds are shown. The disorder has chosen to be strong so that it maximizes the amplitude of the roughness scaling. However, there are still some deviations in the form of greater exponents than the expected from Eq. (14), which gives the value $\psi = 1/2$ and $\psi \simeq 0.26$ in $(1+1)$ and $(2+1)$ dimensions from $\zeta_{(1+1)} = 2/3$ and $\zeta_{(2+1)} = 0.41 \pm 0.01$, respectively. When one has $L \propto L_z$ calculating the average mean height $\langle \overline{z}(h) \rangle$ with a fixed field h is nothing but averaging over the jumped and not jumped interfaces together with their location, Fig. 5(a), in which case $\langle \overline{z}(h) \rangle$ is a good example of a non-self-averaging quantity, see Section 1.2.

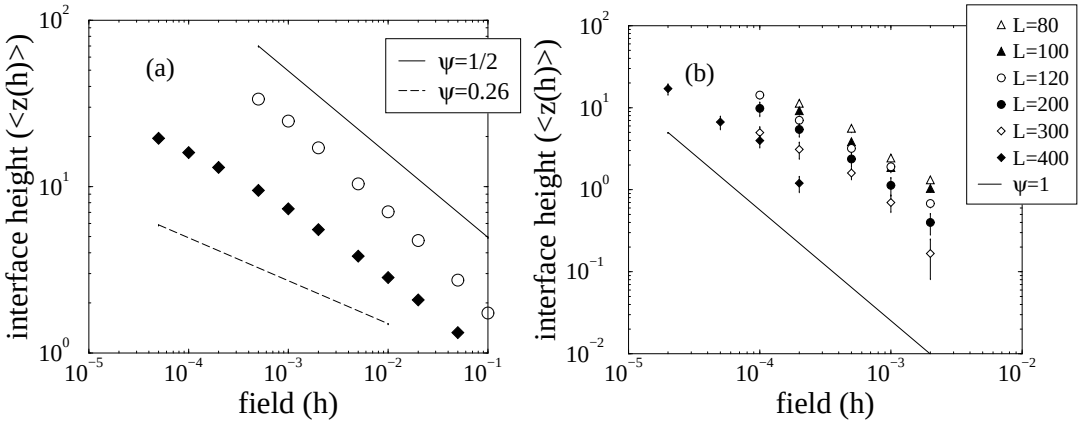

Figure 8: (a) The average interface mean height $\langle \bar{z}(h) \rangle$, as a function of the external field h for one dimensional directed polymers, open circles. The filled diamonds denote $(2+1)$ dimensional interfaces. The solid line is a guide to the eye with a slope $\psi = 1/2$ and the dashed line has a slope $\psi = 0.26$. (b) $\langle \bar{z}(h) \rangle$ vs. h for various system sizes in the flat regime. The line is a guide to the eye with a slope $\psi = 1$.

In Fig. 8(b) the average mean height $\langle \overline{z}(h) \rangle$ versus the field h for $(2+1)$ dimensional manifolds with a weak disorder is plotted. In this case *weak* means for system sizes used that the roughness of the manifold is not yet in the asymptotic roughness limit, $L < L_1$, Eq. (28). The behavior is simple: either the interface stays in its original position or jumps directly

to the wall. Taking into account the jumped and original interfaces as $\langle z(h)\rangle = \langle z[1 - P(\overline{z}_0, h)]\overline{z}_0 + P(\overline{z}_0, h) \times 0\rangle = \langle [1 - P(\overline{z}_0, h)]\overline{z}_0\rangle = \int_0^{L_z} [1 - P\{\overline{z}_0(h)\}]\overline{z}_0\, d\overline{z}_0$ gives the behavior $\langle z(h)\rangle \sim h^{-1}$, *i.e.*, the exponent $\psi \simeq 1$, if $P\{\overline{z}_0(h)\} \sim h^{-1}$. The larger manifolds jump faster to the wall, *i.e.*, they feel the perturbation earlier, since Eq. (38) for flat interfaces ($\zeta = 0$) becomes $\langle h_1(L, L_z)\rangle \sim L^{\theta - D} L_z^{-1} [\ln(L_z)]^{-1/2}$. With fixed L_z and $\theta = D/2$ from Poissonian statistics, in $D = 2$ leads to $\langle h_1(L)\rangle \sim L^{-1}$, which is confirmed in Fig. 8(b). This gives the behavior of the wetting scaling, $\langle \bar{z}(h)\rangle \sim c(L) h^{-\psi}$ where $c(L) \simeq L^{-1}$ and $\psi = 1$. The finite size scaling of the prefactor indicates that at the large L-limit with fixed L_z the flat interfaces are immediately at the wall, and thus the systems are non-wet. This implies that there is cross-over around L_1 between such a "dry" regime and the bulk wetting that takes over for even larger L.

The $(1 + 1)$ dimensional wetting exponent has been confirmed already in an earlier work [92], but the $(2 + 1)$ dimensional studies for rough and flat interfaces are new.

4 Random Field Ising Magnets

Let us turn now from random-exchange magnets to random-field magnets. In Section 4.1 the destruction of the effective ferromagnetic phase in two-dimensional random-field magnets is demonstrated. The domain wall structure and its behavior, when crossing the so called *break-up length scale*, are studied in Section 4.2. Above the break-up length scale, where random field magnets are paramagnetic, the behaviors of the magnetization and the susceptibility are demonstrated, Section 4.3. An interesting phenomenon, a *percolation transition*, in two-dimensional random-field magnets is studied in Section 4.4. All the results are published in the articles VI and VII.

4.1 Destruction of Long Range Order

For small system sizes the random field magnets with weak disorder prefer to be ferromagnetic (FM), *i.e.*, to have a *long-range order*, since the cost of having a domain wall cannot be compensated with the gain from flipping a domain of spins if the domain is not big enough. However, in two dimensions for large enough system sizes the system breaks into domains, as proposed by Imry and Ma, and becomes paramagnetic (PM). The length scale L_b at which this happens is the so called *break-up length scale*, and it depends exponentially on the random field strength squared, Eq. (6). The result has been derived using extreme statistics in Publication VII. It is amusing to note that the optimization of the domain wall by Binder [23] and the optimization of a droplet as a rare phenomenon lead to the same scaling.

It can be easily understood that the most preferable domain is the one which maximizes the area and minimizes the number of bonds to be broken, so that the domain is on the average half the system size. Fig. 9(a) illustrates this, as we increase (with a fixed random field configuration and system size) the strength of the randomness or decrease the ferromagnetic couplings until the first domain appears.

This kind of nucleation with a critical size is reminiscent of a first order transition, and is related to a level-crossing, when either the random field strength or the system size is varied. This is similar to random elastic manifolds, when an extra periodic potential, Section 2.2, or a constant external field, Section 3.1, is applied. The magnetization for a certain disorder strength and system size would be averaged over systems, in which the first

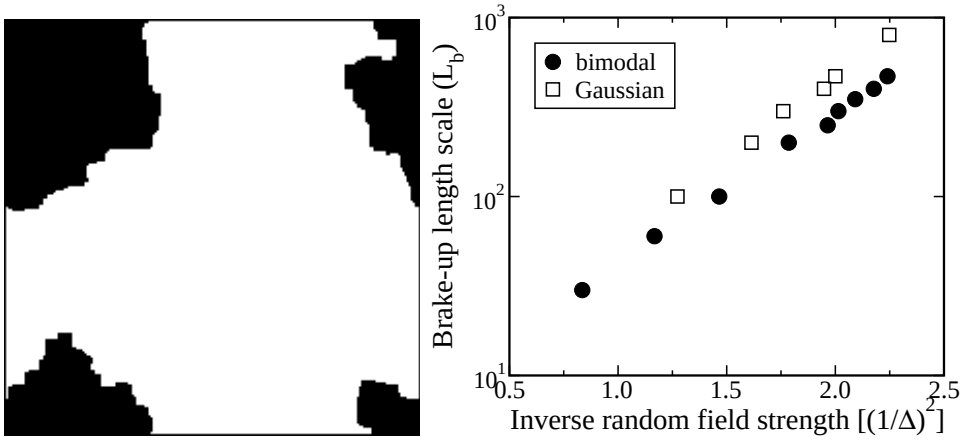

Figure 9: (a) An example of the ground state after the first excitation. "Up" spins are drawn in white, and "down" spins in black. (b) The brake-up length scale L_b versus inverse random field strength $(1/\Delta)^2$ for bimodal and Gaussian disorder (filled circles and empty squares, respectively).

excitation has ($|m| \simeq 0$) and has not ($|m| \simeq 1$) been formed yet. Hence a simpler measure for the break up of FM order is defined: the probability of finding a purely ferromagnetic system, $P_{FM}(L, \Delta)$, *i.e.*, for a fixed random field strength and system size we calculate the probability over several realizations for magnetization $|m| = 1$. If the transition to the PM state would be continuous, this would not make much sense, since already small fluctuations would cause $P_{FM}(L, \Delta) \simeq 0$. However, due to the first-order behavior, and to the fact that the smallest energy needed to flip a domain causes the excitation to be large, P_{FM} is a good measure and has a smooth behavior. We have checked that $|m|$ vs. P_{FM} does not depend on L.

The break-up length scale L_b is derived here by varying the random field strength Δ from the probability of finding a pure ferromagnetic system as $P_{FM}(L_b, \Delta) = 0.5$. The same criterion has been used successfully later in studying the break-up of randomly coupled ferromagnets [93]. The data is shown in Fig. 9(b) for Gaussian and bimodal RF disorder (in both cases $J = 1$), and the exponential scaling for L_b vs. inverse random field strength squared is clearly seen. The prefactors are $A = 2.1 \pm 0.2$ and 1.9 ± 0.2 for Gaussian and bimodal disorder, respectively.

After the ground state is broken to several domains, the largest domains become fractals, see Section 4.4.

4.2 Domain Walls in 2D Random Field Ising Magnets

The scaling properties of domain walls are studied here with the so-called *domain wall renormalization group* (DWRG) method [94]. The Hamiltonian (2) is minimized using boundary conditions, where the spins in opposite boundaries are fixed to be up and down. This is compared to a system with the same disorder, but with periodic boundaries. The energy of creating the domain wall is the difference of the energies of the first, domain wall enforcing, and the second, "normal", case,

$$E_{DW}(L) = E_{fixed}(L) - E_{periodic}(L). \tag{42}$$

Note that when calculating the energy of a domain wall as above it is equal to the differences in the maximum flow, Eq. (16), since the first terms in Eq. (18) in the domain wall enforcing and the periodic cases cancel each other.

In Fig. 10(a) the interface width with respect to the system size for three different disorder strength values is shown. For a weak disorder the global roughness exponent is found to be $\zeta \simeq 1.2 \pm 0.05$ and thus contradicts the RG result $\zeta = (4 - D)/3$. This larger exponent exists only up to the break up length scale, L_b, *i.e.*, when the systems are effective ferromagnetic. Above the break up length scale the domains become fractal and $\zeta = 1$, see Section 4.4. There is a sharp transition between these two regimes and the data for $\Delta = 10/9$ in the inset of Fig. 10(a) has two regimes, one corresponding to the effective ferromagnetic phase and the other to the paramagnetic phase. Driven interface simulations have yielded a large exponent, $\zeta \simeq 1.2 \pm 0.05$, too (see *e.g.* [95]).

In order to understand the behavior of the domain walls with an roughness exponent greater than unity, the interface fluctuations in the form of the interface step height probability density function (pdf) $f(\Delta z_{i,i+1}, L)$ are studied, too. $\Delta z_{i,i+1}$ is the height difference between two neighboring sites (z_i) along the solid-on-solid interface, *i.e.*, the overhangs are neglected (the same behavior is seen even when only the steps are considered, if there are no overhangs). The $f(\Delta z, L)$ shows stretched exponential behavior and the pdf's are clearly L-dependent, but only up to the break up length scale. The data is shown in Publication VI. A similar behavior, so called *turbulent scaling*, is seen in interface growth problems, which are governed by intermittent, rare events [96]. A multi-fractal study, see Section 1.3, of the average step height $|\Delta z|$ and the interface height-height-correlation

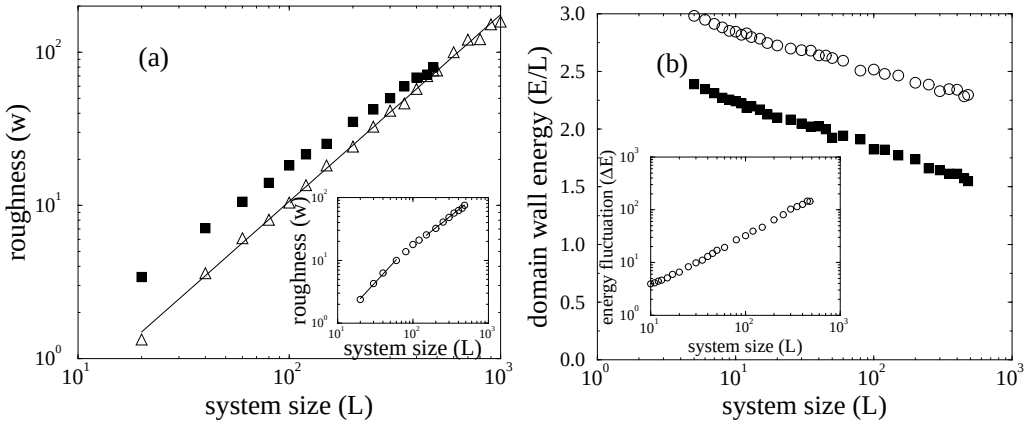

Figure 10: (a) Scaling of the interface width for a bimodal disorder, $\Delta = 2/3$ (empty triangles) and 3/2 (filled squares). The line indicates a least-squares fit with a roughness exponent $\zeta = 1.20 \pm 0.05$. The inset shows the cross-over in interface properties with increasing system size ($\Delta = 10/9$). (b) Scaling of the energy (per length) for bimodal $\Delta = 1/3$ (empty circles) and 5/12 (filled squares). The inset shows the scaling of energy fluctuations for $\Delta = 1/3$.

functions $G_k(r)$ demonstrates a multi-affine behavior in the local interface scaling. The first and the second moments of the height-height-correlation functions have exponents $\alpha_1 \simeq 0.88$ and $\alpha_2 \simeq 0.66$, respectively. The latter exponent is seen for RF domain wall scaling with an external field, too [97].

Fig. 10(b) shows the DWRG result for the domain wall energy: there is a logarithmic correction to the domain wall energy in the FM "phase", as proposed by Binder in his domain wall optimization calculation when calculating L_b, see Publication VII. In the PM phase the energy has only a remnant contribution from the boundary conditions. It should be noted that the behavior does not depend on the type of disorder, but is similar for both the bimodal and the Gaussian distributions. For the FM "phase" the energy fluctuation exponent is $\theta \simeq 1$, see the inset of Fig. 10(b). The values for the exponents ζ and θ below L_b disagree with the exponent relation, Eq. (11).

The different interface roughness scaling behaviors for system sizes below and above L_b indicate that the domain wall roughening is not scale invariant. Since the interface stiffness vanishes at L_b and there is a violation of the hyper-scaling relation, the RG phase diagrams proposed for the DP/KPZ

problem with the correlated disorder [98, 99] fail at this point.

4.3 Magnetization and Susceptibility of 2D Random Field Ising Magnets

The external field response to the ground states of two-dimensional random field magnets is studied in this Section using the Gaussian distribution for the random fields. There is a constant external field H applied to the magnet, which adds the term $-H\sum_i S_i$ in the Hamiltonian (2). Adding an external field to the systems, whose system sizes are above the break-up length scale, L_b, does not lead to a first-order type of behavior, similarly to the first Imry-Ma -domains, but the domains melt continuously, Publication VII. Below L_b in effective ferromagnetic systems an "avalanche" like behavior could be studied [100], but because the effective ferromagnetism vanishes for large enough system sizes and thus does not exist at the thermodynamic limit, that behavior is not interesting.

The magnetization behaves continuously and all the magnetization values for different system sizes lie exactly on top of each other, when $L > L_b$, at least if the statistics is good. In order to find the scaling between the external field and the random field strength the crossing points of magnetization curves with a fixed magnetization values at external fields H_m are taken for different random field strength values Δ. The external field H_m scales exponentially with respect to the random field strength,

$$H_m \sim \exp(-6.5/\Delta). \tag{43}$$

The data-collapse using the scaling (43) is shown in Fig. 11(a) confirming the scaling. The magnetization behaves linearly with respect to the external field for small field values H and has exponential tails. The exponential behavior of Eq. (43) implies that there is a unique "melting rate" at which the cluster boundaries get eroded as H increases and that the process is otherwise similar for all Δ.

Also the susceptibility, $\chi \sim \langle m^2 - \langle m \rangle^2 \rangle$, with respect to the external field is studied. The susceptibility is shown to vanish with respect to the area of the systems, $\chi \sim L^{-2}$, Publication VII. In Fig. 11(b) the susceptibility versus the external field has been data-collapsed by scaling the external field with (43) (as for magnetization) and the susceptibility with $\chi \sim \exp(7.3/\Delta)$.

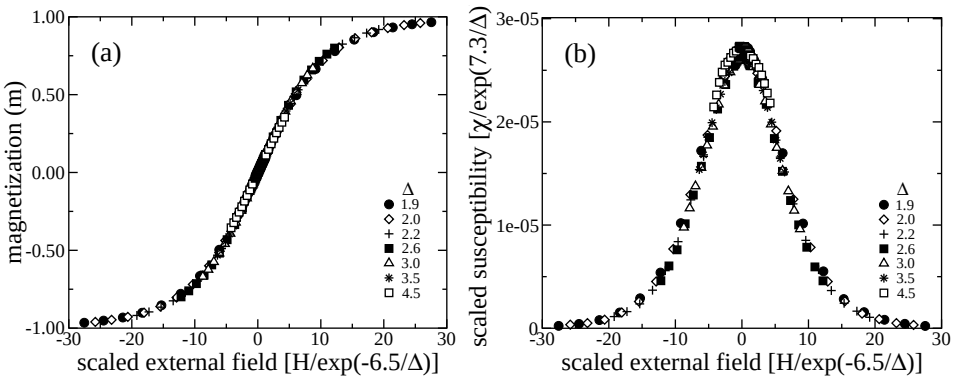

Figure 11: (a) The data-collapse of the magnetization m versus the scaled external field $H/\exp(-6.5/\Delta)$ for various random field strength values. (b) The scaled susceptibility $\chi/\exp(7.3/\Delta)$ versus the scaled external field $H/\exp(-6.5/\Delta)$ for several random field strength values.

The shape of the data-collapse is constant for small external field values H and has exponential tails for large values. This seem to result from the magnetization through $\chi = \partial m/\partial H$. To summarize the behavior of the susceptibility

$$\chi \sim L^{-2} \exp(7.3/\Delta) g(H/H_m), \tag{44}$$

where H_m is from Eq. (43) and

$$g(y) \sim \begin{cases} \text{const}, & y \simeq 0, \\ \exp(-0.2|y|), & y \to \pm\infty. \end{cases} \tag{45}$$

From the susceptibility one gets the magnetization correlation length ξ_m, which thus has an exponential dependence on the random field strength and is not related to the L_b.

The continuous behaviors for the magnetization and the susceptibility are consistent with the Aizenman-Wehr argument proving the nonexistence of ferromagnetism in 2D RFIM [27] and indicate that the proposals for a critical random field strength value or a phase transition are wrong [101].

4.4 Percolation in 2D Random Field Ising Magnets

Above the break up length scale L_b the domains look like fractals. Actually, they resemble percolation clusters by having domains inside domains and

they are of all different sizes, even up to the system size [47]. Thus the percolation behavior in two-dimensional random field Ising magnets is studied here.

When the random field strength is well above the coupling constant value, $\Delta \gg J$, the percolation can be easily understood by considering it as an ordinary site-occupation problem. This means that only the random field directions are important and the coupling constants may be neglected. The site-percolation occupation threshold probability for square-lattices is $p_c \simeq 0.593$ [47], *i.e.*, well above one half. Applied to the strong random field strength case it means that there must be a finite external field in order to get a domain spanning the system. However, when the random field strength is decreased, the coupling constants start to contribute and in some cases a domain spans the system even without an external field. Hence, we propose a phase-diagram, Fig. 12(a).

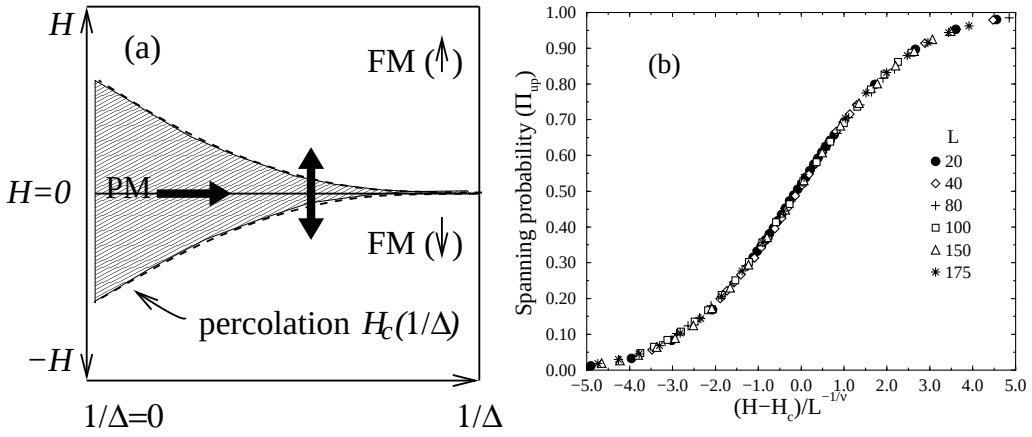

Figure 12: (a) The phase diagram for the 2D RFIM with disorder strength Δ and an applied external field H. The $1/\Delta = 0$ axis corresponds to the standard site-percolation, with the percolation occupation fraction $p_c = 0.593$. The dashed lines define the percolation thresholds $H_c(1/\Delta)$ for up and down spins, below and above of which the systems are simple ferromagnetic. (b) The data-collapse using $L^{-1/\nu}$, $\nu = 4/3$ and $H_c = 0.00186 \pm 0.0008$ for up spin-spanning Π_{up} as a function of H for $\Delta = 2.6$.

The spanning probabilities of up spins Π_{up} with respect to the external field H for several system sizes L, which are greater than L_b, and for a number of random field strength values have been studied in the direction of the vertical arrow in Fig. 12(a). Using the correlation length exponent of the

standard percolation, $\nu = 4/3$ [47], the critical external field has been estimated to be $H_c = 0.00186$ for $\Delta = 2.6$ and the data-collapse of Π_{up} versus $(H - H_c)/L^{-1/\nu}$ is shown in Fig. 12(b), which confirms the estimates of H_c and $\nu = 4/3$. Similar data-collapses for various other random field strength values Δ can be obtained as well. In order to test further the universality class of the percolation transition studied here also the order parameter of the percolation, the probability of belonging to the up-spin spanning cluster P_∞, is calculated. The data-collapse of $P_\infty/L^{-\beta/\nu}$, $\beta = 5/36$, $\nu = 4/3$ versus the scaled external field $(H - H_c)/L^{-1/\nu}$ has been successfully attempted, Publication VII. The fractal dimension of the spanning cluster has been measured and the mass of the spanning cluster, as the sum of the random fields in it, scales with the same fractal dimension $D_f = 91/48$ as the standard short-range correlated two-dimensional percolation. Thus the percolation transition with respect to the external field is in the standard short-range correlated percolation universality class [47] and there exists a percolation correlation length ξ_{perc}, which diverges with a correlation length exponent $\nu = 4/3$. This, together with L_b, should explain different correlation lengths found for 2D RFIM [102]. The standard correlation universality class is not surprising, since all two-dimensional short-range correlated percolation systems belong to the same universality class. Although the ground state structure originates from global optimization, the correlations in the system are not long-range. Other exponents could be measured, too, as γ for the average size $\langle s \rangle$ of the clusters, and σ and τ for the cluster size distribution. Note, however, that one must be above the break up length scale and the control parameter should be the external field H instead of the disorder strength Δ in order to get the correct exponents. In an earlier work the cluster size distribution has been measured at $H = 0$ giving an exponent differing from standard percolation [103]. This is because for the used Δ $H_c \gg 0$.

There is, however, another question: do the percolation lines in Fig. 12(a) meet each other at finite Δ_c, *i.e.*, does there exist a spanning cluster also when $H = 0$ and $\Delta > 0$? In order to answer the question a critical type of scaling using the calculated H_c for various Δ has been attempted. The Ansatz is

$$H_c \sim (\Delta - \Delta_c)^\delta, \tag{46}$$

where $\delta = 2.05 \pm 0.10$. In Fig. 13(a) the calculated Δ values versus the scaled critical external field $[H_c(\Delta)]^{1/2.05}$ is plotted and it gives the estimate

$\Delta_c = 1.65 \pm 0.05$. This indicates that the percolation probability lines for up and down spins meet at $\Delta_c = 1.65$ and for Δ below the critical Δ_c there is always spanning of either of the spin directions in the systems, even for $H = 0$. Actually one should note, that the only way that neither of the spin directions span is to have a so called checker-board situation, which prevents both of the spin directions to have neighbors with the same spin orientation. However, another scenario with an exponential behavior for $H_c(\Delta)$ fits to the data reasonably well. This would suggest, that there is no finite Δ_c. Fig. 13(b) shows a behavior of $H_c \sim \Delta^2 \exp(-13/\Delta^2 - 4)$. If this scaling is correct, then the effective percolation seen at finite system sizes vanishes at the critical length scale L_c which is large enough that one can be below it in experiments, and thus a system can "apparently percolate".

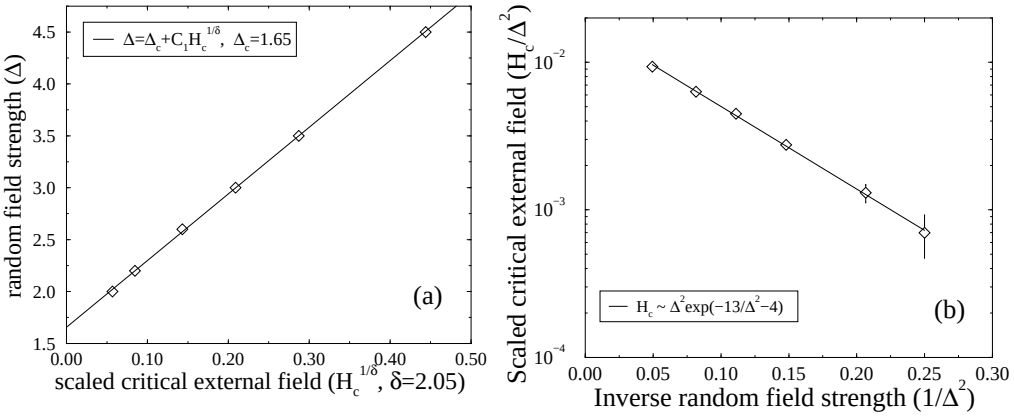

Figure 13: (a) The critical $[H_c(\Delta)]^{1/\delta}$, where $\delta = 2.05 \pm 0.10$, of up spin -spanning for each Δ. The data follows $H_c \sim (\Delta - \Delta_c)^{\delta}$, where $\Delta_c = 1.65 \pm 0.05$. (b) The other scenario with $H_c \sim \Delta^2 \exp(-13/\Delta^2 - 4)$.

The percolation transition has been also studied at $H = 0$ and varying Δ, Publication VII, but it is much harder to define, since when moving in the direction of the horizontal arrow in Fig. 12(a) the critical lines of up and down spanning are approaching and interfering with each other. Also, the so called *red clusters* (RC) have been studied. They are like red sites in the standard percolation, so that removing any single one breaks up the spanning cluster. In this case it is investigated what happens if one inverts any spin belonging to the spanning cluster by fixing the local field h_i to a large value opposite to the spin orientation. Then the new ground state is found. The crucial difference to site-percolation is that now a whole sub-cluster can be reversed. It is investigated whether the original cluster

retains its spanning property for each spin or trial cluster in analogy with ordinary percolation. Those spins that lead to a destructive (cluster) flip define then *red clusters* as all the spins that reversed simultaneously. The finite size scaling of the number of the red clusters, $\langle N_{RC} \rangle$, is shown to scale with $L^{1/\nu}$, where $\nu \simeq 4/3$ as in ordinary percolation for red sites, for field values $\Delta \leq \Delta_c$, when $L > L_b$. The amplitude for the scaling of $\langle N_{RC} \rangle$ is larger the smaller the field, as is the average mass of red clusters $\langle M_{RC} \rangle$. $\langle M_{RC} \rangle$ is independent of the system size L and depends only on the random field strength Δ, Publication VII.

The percolation transition in 2D RFIM explains the problems met when characterizing the structure of the ground states: why the susceptibility seems to be diverging at $H = 0$ and seems to suggest a transition from a paramagnetic to a ferromagnetic phase [101], which is in contradiction to the Aizenman-Wehr argument [27]. The percolation lines have an effect at finite system sizes when the system size L is below the correlation length ξ, also for higher Δ than the percolation Δ_c. Introducing the external field in the system makes the whole picture simpler and enables to distinguish the geometric from the magnetic properties of the ground states of random field magnets. The average mass of red clusters defines an estimate for the length scale over which the spins are correlated. Since $\langle M_{RC} \rangle$ is not system size dependent, at large enough length scales the correlations are renormalized to be short-ranged, and thus the whole ground state of the random field Ising magnet is short-range correlated except when it is geometrically correlated due to the percolation.

5 Conclusions

In this thesis elastic manifolds, in the presence of either of two different types of periodicity or an external field, and the ground states of random field Ising magnets are studied at zero temperature using exact ground state calculations and extreme statistics arguments. The graph-theoretical combinatorial optimization method is shown to be an accurate and powerful tool in studying numerically the ground states of random magnets. The extreme statistics is a useful method in analyzing the first excitations in systems with a complex energy landscape. It has been actively used lately in various other physical applications in which usual self-averaging does not apply [87, 104, 105, 106, 107, 108].

The elastic manifolds with an additional sinusoidal potential are shown to exhibit chaos type of behavior, similar to spin glasses [109], by moving with sharp jumps between the minima of the periodic potential. The roughening cross-over when tuning the system size or the amplitude of the periodic potential is demonstrated to have a first-order-like transition [58].

The applied external field in the random manifolds are shown in $T = 0$ to move by sharp jumps between nearly degenerate minima. However, the relevance of this to the creep phenomenon at small, finite temperatures is still unclear and needs more study [54, 110]. The zero-temperature susceptibility is shown to be dependent on the scaling of the number of the nearly degenerate energy minima in the system, in contrast to calculations based on smooth continuous behavior [71].

The ground states of random field magnets are demonstrated to break up at the length scale predicted by Binder [23] and not to have any phase transition [101] contradicting the Aizenman-Wehr argument [27]. The first-order character seen in the break-up of the two-dimensional random field magnets may be related to the discussion of the three-dimensional case [111, 112, 113]. Domain walls in random magnets exhibit a multi-scaling behavior and a roughness exponent higher than the renormalization group calculations suggest [44]. It will be interesting to see if this phenomenon exists in higher dimensions, too. The percolation transition studied for the random field magnets explains the difficulties in understanding the ground state structure of random field magnets [101, 102] and may be related to the percolation hull exponent seen in dynamical, non-equilibrium simulations [114, 115].

References

[1] J. Cardy, *Scaling and Renormalization in Statistical Physics* (Cambridge University Press, Cambridge, UK, 1996).

[2] J. M. Yeomans, *Statistical Mechanics of Phase Transitions* (Oxford University Press, Oxford, UK, 1992).

[3] N. Goldenfeld, *Lectures on Phase Transitions and Renormalization Group* (Addison-Wesley, Reading, Massachusetts, 1995).

[4] Y. Imry and S.-k. Ma, Phys. Rev. Lett. **35**, 1399 (1975).

[5] D. S. Fisher, G. M. Grinstein, and A. Kuharana, Physics Today **41** (12), 56 (1988).

[6] Brush S. G., Rev. Mod. Phys. **39**, 883 (1967).

[7] M. Mézard, G. Parisi, and M. A. Virasoro, *Spin Glass Theory and Beyond* (World Scientific, Singapore, 1987).

[8] K. Binder and A. P. Young, Rev. Mod. Phys. **58**, 801 (1986).

[9] P. Nordblad and P. Svedlindh, in *Spin Glasses and Random Fields*, edited by A. P. Young (World Scientific, Singapore, 1997).

[10] D. P. Belanger and A. P. Young, J. Magn. Magn. Mater. **100**, 272 (1991).

[11] T. Nattermann, in *Spin Glasses and Random Fields*, edited by A. P. Young (World Scientific, Singapore, 1997).

[12] S. Fishman and A. Aharony, J. Phys. C **12**, L729 (1979).

[13] J. L. Cardy, Phys. Rev. B **29**, R505 (1984).

[14] D. P. Belanger, in *Spin Glasses and Random Fields*, edited by A. P. Young (World Scientific, Singapore, 1997).

[15] R. Blossey, T. Kinoshita, X. Müller, and J. Dupont-Roc, J. Low Temp. Phys. **110**, 665 (1998).

[16] G. Grinstein, Phys. Rev. Lett. **37**, 944 (1976).

[17] A. Aharony, Y. Imry, and S-k. Ma, Phys. Rev. Lett. **37**, 1367 (1976).

[18] A. P. Young, J. Phys. C **10**, L257 (1977).

[19] G. Parisi and N. Sourlas, Phys. Rev. Lett. **43**, 744 (1979).

[20] K. Binder, Y. Imry, and E. Pytte, Phys. Rev. B **24**, 6736 (1981).

[21] G. Grinstein and S-k. Ma, Phys. Rev. Lett. **49**, 685 (1982).

[22] G. Grinstein and S-k. Ma, Phys. Rev. B **28**, 2588 (1983).

[23] K. Binder, Z. Phys. B **50**, 343 (1983).

[24] T. Nattermann, Z. Phys. B **54**, 247 (1984).

[25] J. Z. Imbrie, Phys. Rev. Lett. **53**, 1747 (1984).

[26] J. Bricmont and A. Kupiainen, Phys. Rev. Lett. **59**, 1829 (1987).

[27] M. Aizenman and J. Wehr, Phys. Rev. Lett. **62**, 2503 (1989).

[28] A. B. Harris, J. Phys. C **7**, 1671 (1974).

[29] J. Villain, Phys. Rev. Lett. **52**, 1543 (1984).

[30] G. Grinstein and J. Fernandez, Phys. Rev. B **29**, 6389 (1984).

[31] L. Balents, Lecture notes, the Beg-Rohu spring school (1996).

[32] T. Giamarchi and P. Le Doussal, in *Spin Glasses and Random Fields*, edited by A. P. Young (World Scientific, Singapore, 1997).

[33] L. Balents and D. S. Fisher, Phys. Rev. B **48**, 5949 (1993).

[34] T. Emig and T. Nattermann, Europhys. J. B, **8** 525, (1999).

[35] T. Halpin-Healy and Y.-C. Zhang, Phys. Rep. **254**, 215 (1995).

[36] G. Blatter, M. V. Feigel'man, V. B. Geshkenbein, A. I. Larkin, and V. M. Vinokur, Rev. Mod. Phys. **66**, 1125 (1994).

[37] J. Kertész, V. K. Horváth, and F. Weber, Fractals **1**, 67 (1993).

[38] A. Hansen, E. L. Hinrichsen, and S. Roux, Phys. Rev. Lett. **66**, 2476 (1991).

[39] E. T. Seppälä, V. I. Räisänen, and M. J. Alava, Phys. Rev. E **61**, 6312 (2000).

[40] V. I. Räisänen, E. T. Seppälä, M. J. Alava, and P. M. Duxbury, Phys. Rev. Lett. **80**, 329 (1998).

[41] E. Hopf, Comm. Pure Appl. Math. **3**, 201 (1950); J. D. Cole, Quart. Appl. Math. **9**, 225 (1951).

[42] M. Kardar, G. Parisi, and Y.-C. Zhang, Phys. Rev. Lett. **56**, 889 (1986).

[43] M. Kardar, Lecture notes, Les Houches Summer School (1994); cond-mat/9411022.

[44] D. Fisher, Phys. Rev. Lett. **56**, 1964 (1986).

[45] G. Forgacs, R. Lipowsky, and Th. M. Nieuwenhuizen, in *Phase Transitions and Critical Phenomena*, edited by C. Domb and J. L. Lebowitz (Academic Press, San Diego, 1991), vol. 14.

[46] A.-L. Barabási and H. E. Stanley, *Fractal concepts in surface growth* (Cambridge University Press, Cambridge, U.K., 1995).

[47] D. Stauffer and A. Aharony, *Introduction to Percolation Theory* (Taylor & Francis, London, 1994).

[48] A.-L. Barabási, R. Bourbonnais, M. Jensen, J. Kertész, T. Vicsek, and Y.-C. Zhang, Phys. Rev. A **45**, R6951 (1992).

[49] P. Meakin, *Fractals, scaling, and growth far from equilibrium* (Cambridge University Press, Cambridge, U.K., 1998).

[50] D. A. Huse and C. L. Henley, Phys. Rev. Lett. **54**, 2708 (1985).

[51] D. S. Fisher and D. A. Huse, Phys. Rev. B **43**, 10 728 (1991).

[52] S. Scheidl and Y. Dinçer, cond-mat/0006048.

[53] P. Chauve, P. Le Doussal, and K. Wiese, Phys. Rev. Lett. **86**, 1785 (2001).

[54] P. Chauve, T. Giamarchi, and P. Le Doussal, Phys. Rev. B **62**, 6241 (2000).

[55] G. Parisi, J. Phys. France **51**, 1595 (1990).

[56] J.-Ph. Bouchaud and A. Georges, Phys. Rev. Lett. **68**, 3908 (1992).

[57] T. Emig and T. Nattermann, Phys. Rev. Lett. **81**, 1469 (1998).

[58] A. Hazareesing and J.-Ph. Bouchaud, Phys. Rev. Lett. **81**, 5953 (1998); T. Emig and T. Nattermann, Phys. Rev. Lett. **81**, 5954 (1998);

[59] J. L. Cardy and S. Ostlund, Phys. Rev. B **25**, 6899 (1982).

[60] J. Toner and D. P. DiVincenzo, Phys. Rev. B **41**, 632 (1990).

[61] Y. C. Tsai and Y. Shapir, Phys. Rev. Lett. **69**, 1773 (1992).

[62] H. Rieger, Phys. Rev. Lett. **74**, 4964 (1995).

[63] C. Zeng, A. A. Middleton, and Y. Shapir, Phys. Rev. Lett. **77**, 3204 (1996).

[64] H. Rieger and U. Blasum, Phys. Rev. B **55**, R7394 (1997).

[65] C. Zeng, J. Kondev, D. McNamara, and A. A. Middleton, Phys. Rev. Lett. **77**, 109 (1998).

[66] R. Lipowsky and M. E. Fisher, Phys. Rev. Lett. **56**, 472 (1986).

[67] J. Wuttke and R. Lipowsky, Phys. Rev. B **44**, 13 042 (1991).

[68] S. Dietrich, in *Phase Transitions and Critical Phenomena*, edited by C. Domb and J. L. Lebowitz (Academic Press, San Diego 1988), vol. 12.

[69] M. Mézard, J. Phys. France **51**, 1831 (1990).

[70] T. Hwa and D. S. Fisher, Phys. Rev. B **49**, 3136 (1994).

[71] Y. Shapir, Phys. Rev. Lett. **66**, 1473 (1991).

[72] M. Alava, P. Duxbury, C. Moukarzel, and H. Rieger, in *Phase Transitions and Critical Phenomena*, edited by C. Domb and J. L. Lebowitz (Academic Press, San Diego, 2001), vol 18.

[73] H. Rieger, *Lecture Notes in Physics 501* (Springer-Verlag, Heidelberg, 1998).

[74] J. C. Picard and H. D. Ratliff, Networks **5**, 357 (1975)

[75] F. Barahona, J. Phys. A **18**, L673 (1985).

[76] J. C. Anglès d'Auriac, M. Preissmann, R. Ramal, J. de Physique Lett. **46**, L173 (1985).

[77] A. T. Ogielski, Phys. Rev. Lett. **57**, 1251 (1986).

[78] L. R. Ford and D. R. Fulkerson, *Flows in Networks* (Princeton University Press, Princeton, 1962).

[79] A. V. Goldberg and R. E. Tarjan, J. Assoc. Comput. Mach. **35**, 921 (1988).

[80] E. Seppälä, *Scaling of Minimum Energy Interfaces* (Master's Thesis, Helsinki University of Technology, 1996).

[81] R. Ahuja, T. Magnanti, and J. Orlin, *Network Flows* (Prentice Hall, New Jersey, 1993).

[82] M. Kardar and Y.-C. Zhang, Phys. Rev. Lett. **58**, 2087 (1987).

[83] J. Galambos, *The Asymptotic Theory of Extreme Order Statistics* (John Wiley & Sons, New York, 1978).

[84] J.-Ph. Bouchaud and M. Mézard, J. Phys. A **30**, 7997 (1997).

[85] J. A. Kim, M. A. Moore, and A. J. Bray, Phys. Rev. A **44**, 2345 (1991).

[86] E. J. Gumbel, *Statistics of Extremes*, (Columbia University Press, New York, 1958).

[87] S. Chapman, G. Rowlands, and N. Watkins, cond-mat/0007275.

[88] Y.-C. Zhang, Phys. Rev. Lett. **59**, 2125 (1987).

[89] T. Natterman, Phys. Rev. Lett. **60**, 2701 (1988); Y.-C. Zhang, Phys. Rev. Lett. **60**, 2702 (1988); M. V. Feigel'man and V. M. Vinokur, Phys. Rev. Lett. **61**, 1139 (1988); Y.-C. Zhang, Phys. Rev. Lett. **61**, 1139 (1988).

[90] M. J. Alava and P. M. Duxbury, Phys. Rev. B **54**, 14990 (1996).

[91] L. Balents, J.-Ph. Bouchaud, and M. Mézard, J. Phys. I **6**, 1007 (1996).

[92] M. Huang, M. E. Fisher, and R. Lipowsky, Phys. Rev. B **39**, 2632 (1989).

[93] A. K. Hartmann and I. A. Campbell, Phys. Rev. B **63**, 094423 (2001).

[94] W. L. McMillan, Phys. Rev. B **29**, 4026 (1984).

[95] H. Leschhorn, Physica A **195**, 324 (1993).

[96] J. Krug, Phys. Rev. Lett. **72**, 2907 (1994).

[97] M. Jost, J. Esser, and K. D. Usadel, Phys. Stat. Sol. B **202**, R11 (1997).

[98] Y.-C. Zhang, J. Phys. A **19**, L941 (1986).

[99] E. Frey, U. C. Täuber, and H. K. Janssen, Europhys. Lett. **47**, 14 (1999).

[100] C. Frontera and E. Vives, Phys. Rev. E **62**, 7470 (2000).

[101] C. Frontera and E. Vives, Phys. Rev. E **59**, R1295 (1999).

[102] S. L. A. de Queiroz and R. B. Stinchcombe, Phys. Rev. E **60**, 5191 (1999).

[103] J. Esser, U. Nowak, and K. D. Usadel, Phys. Rev. B **55**, 5866 (1997).

[104] Ch. Texier, J. Phys. A **33**, 6095 (2000).

[105] S. Datta and S. Redner, Phys. Rev. Lett. **84**, 6018 (2000).

[106] M. Z. Bazant, Phys. Rev. E **62**, 1660 (2000).

[107] P. L. Krapivsky and S. N. Majumdar, Phys. Rev. Lett. **85**, 5492 (2000).

[108] R. Mohayaee, A. L. Stella, and C. Vanderzande, cond-mat/0101091.

[109] D. S. Fisher and D. A. Huse, Phys. Rev. Lett. **56**, 1601 (1986).

[110] S. Lemerle, J. Ferré, C. Chappert, V. Mathet, T. Giamarchi, and P. Le Doussal, Phys. Rev. Lett. **80**, 849 (1998).

[111] J.-C. Angles-d'Auriac and N. Sourlas, Europhys. Lett. **39**, 473, (1997).

[112] A. K. Hartmann and U. Nowak, Eur. Phys. J. B **7**, 105 (1999).

[113] N. Sourlas, Comp. Phys. Comm. **121-122**, 183 (1999).

[114] H. Ji and M. O. Robbins, Phys. Rev. A **44**, 2538 (1991).

[115] B. Drossel and K. Dahmen, Eur. Phys. J. B **3**, 485 (1998).